Differentiation of Ischemic vs Non-Ischemic Cardiomyopathy by Oxygen-Sensitive Cardiovascular Magnetic Resonance (DINO)

By
Sabri Conde-Yassin

Division of Experimental Medicine
Faculty of Medicine and Health Sciences
McGill University, Montreal

May 31, 2022

A traditional format thesis submitted to McGill University in partial fulfillment of the requirements of the degree of M.Sc. in Experimental Medicine – Thesis.

Table of Contents

1. TABLE OF ABBREVIATIONS

AHA	American Heart Association
B-MORE	Breathing-Induced Myocardial Oxygenation Reserve
BH	Breath Hold
BMI	Body Mass Index
BSA	Body Surface Area
CAD	Coronary Artery Disease
CTCA	Computed Tomography Coronary Angiography
CTTH	Capillary Transit Time Heterogeneity
CMR	Cardiovascular Magnetic Resonance
DINO	Differentiation of Ischemic vs Non-Ischemic Cardiomyopathy via OS-CMR
HF	Heart Failure
HFimpEF	Heart Failure with Improved Ejection Fraction
HFmrEF	Heart Failure with Mildly Reduced Ejection Fraction
HFrEF	Heart Failure with Reduced Ejection Fraction
HFpEF	Heart Failure with Preserved Ejection Fraction
IC	Insuffisance Cardiaque
ICC	Intraclass Correlation Coefficient
ICM	Ischemic Cardiomyopathy
INOCA	Ischemia with No Obstructive Coronary Arteries
IHF	Ischemic Heart Failure
LGE	Late Gadolinium Enhancement
LVEF	Left Ventricular Ejection Fraction
MBF	Myocardial Blood Flow
NICM	Non-Ischemic Cardiomyopathy
OS-CMR	Oxygenation-Sensitive Cardiovascular Magnetic Resonance
P	Probability Value
PET	Positron Emission Tomography
RF	Radiofrequency
ROC	Receiver Operating Characteristic

ROS	Respiratory OS-CMR
SI	Signal Intensity

2. ACKNOWLEDGEMENTS

This work, the body of knowledge is it is built upon, and the clinical and research efforts that allowed for its production are a result of the collaboration, diligence, and generosity of many individuals. I am grateful for the support and devotion of our entire team at the Courtois Cardiovascular Magnetic Resonance Research group.

A special thank you to my supervisor Dr. Matthias G. Friedrich for fostering a research culture fueled by curiosity, creativity, and collaboration. Thank you for providing me the space and support to learn and experiment, and for pushing me to be more. My gratitude is also extended towards to Drs. Elizabeth Hillier, Judy Luu, and Ria Garg for your support, encouragement, and kind friendship, as well as my fellow students Jason Covone, Katarina Eyre, Dr. Mahya Khaki, Kate Lindsay, Mayssa Moukarzel, and Saad Razzaq.

Thank you also to my thesis advisory committee for providing guidance and support to this study: Drs. Mitchel Benovoy, Matthias Friedrich, Nadia Giannetti, and Emily McDonald.

3. ABSTRACT (ENGLISH)

Differentiation of ischemic (ICM) vs non-ischemic (NICM) cardiomyopathy as the underlying cause of heart failure (HF) has important implications for treatment and prognosis. Clinical guidelines continue to rely on diagnostic tools that are invasive, and/or expose HF patients to ionizing radiation, pharmacological stress, or contrast agents to achieve this differentiation. Oxygenation-Sensitive Cardiovascular Magnetic Resonance (OS-CMR) imaging paired with a vasoactive breathing maneuver is a non-invasive, radiation- and needle-free imaging technique, which can measure dynamic global and regional conditions of tissue oxygenation in the myocardium. This proof-of-concept study investigated the capability of established and novel respiratory OS-CMR (ROS) biomarkers to differentiate between ICM and NICM.

In a retrospective investigation of 20 ICM and 13 NICM patients that underwent ROS between 2019 and 2022, we measured normalized signal intensity (SI) values across the breath-hold portion of ROS to assess global and regional myocardial oxygenation dynamics. In analysis of global markers, we found decreased global percent change, slope, standard deviation, and increased slope of standard deviation across the BH in ICM compared to NICM. However, none of these differences were statistically significant (p-value <0.05) in a Student's t-test. In analysis of regional markers, we found decreased minimum segment change, segment range, and minimum coronary territory change, and increased coronary territory range across the breath hold in ICM, compared to NICM. Similarly, no significant differences existed in regional SI dynamics between ICM and NICM groups using a Student's T-test. Of interest, we found that if we treated global percent change and minimum coronary territory change as binomials for positive or negative change, both significantly differentiated between ICM and NICM in chi-square statistic ($p <0.02$, $p<0.03$, respectively). In receiver operating characteristic (ROC) analyses, two biomarkers, along with the slope of standard deviation, achieved an area under the curve nearing the acceptable range (0.7-0.8) of diagnostic utility.

This study was the first to explore a set of novel global and regional markers using normalized SI values obtained by a completely non-invasive imaging technique with OS-CMR, in addition to being the first OS-CMR study to investigate myocardial oxygenation differences between ICM

and NICM patients. As a proof-of-concept study, our results suggest that a future prospective study with a larger sample size may demonstrate the clinical utility of OS-CMR, specifically using multi-parametric analysis tools, as a needle-free means to identify and characterize ischemic cardiomyopathy in HF patients.

4. RÉSUMÉ (FRANÇAIS)

La différenciation d'une cardiomyopathie ischémique (ICM) ou non ischémique (NICM) comme cause sous-jacente de l'IC a des implications importantes pour le traitement et le pronostic. Les directives cliniques continuent de s'appuyer sur des outils de diagnostic invasifs et/ou exposant les patients à des rayonnements ionisants, à un stress pharmacologique ou à des agents de contraste pour parvenir à cette différenciation. L'imagerie par résonance magnétique cardiovasculaire sensible à l'oxygénation (OS-CMR) associée à une manœuvre de respiration vasoactive est une technique d'imagerie non invasive, sans rayonnement ni aiguille, qui peut mesurer les conditions globales et régionales dynamiques de l'oxygénation des tissus dans le myocarde. Cette étude de preuve de concept a examiné la capacité des biomarqueurs respiratoires OS-CMR (ROS) établis et nouveaux à différencier l'ICM et le NICM.

Dans une enquête rétrospective sur 20 patients ICM et 13 patients NICM ayant subi une ROS entre 2019 et 2022, nous avons effectué une analyse des valeurs d'intensités de signaux normalisés sur la partie en apnée de la ROS pour évaluer la dynamique globale et régionale de l'oxygénation myocardique. Dans l'analyse des marqueurs globaux, nous avons constaté une diminution globale du pourcentage de changement, de la pente, de l'écart type et une augmentation de la pente de l'écart type à travers l'apnée dans l'ICM par rapport au NICM. Aucune de ces différences n'était statistiquement significative dans le test T de Student. Dans l'analyse des marqueurs régionaux, nous avons constaté une diminution du changement de segment minimum, de la gamme de segments et du changement de territoire coronaire minimum, et une augmentation de la gamme de territoire coronaire à travers l'apnée dans l'ICM par rapport au NICM. De même, aucune différence significative (valeur p <0.05) n'existait dans la dynamique SI régionale entre les groupes ICM et NICM en utilisant le test T de Student. Fait intéressant, nous avons constaté que si nous traitions

le pourcentage de changement global et le changement de territoire coronaire minimal comme des binômes pour un changement positif ou négatif, les deux différenciaient entre l'ICM et le NICM avec une statistique du chi carré significative ($p < 0,02$, $p < 0,03$, respectivement). Dans les analyses des caractéristiques de fonctionnement du récepteur, deux biomarqueurs ainsi que la pente de l'écart type ont atteint la zone sous les valeurs de la courbe se rapprochant de la plage acceptable (0.7-0.8) d'utilité diagnostique.

Cette étude a été la première à explorer un ensemble de nouveaux marqueurs globaux et régionaux utilisant des valeurs SI normalisées obtenues par une technique d'imagerie totalement non invasive avec OS-CMR, en plus d'être la première étude OS-CMR à étudier les différences d'oxygénation myocardique. entre les patients ICM et NICM. En tant qu'étude de preuve de concept, nos résultats suggèrent qu'une future étude prospective avec un échantillon plus important pourrait potentiellement démontrer la valeur clinique de l'OS-CMR en tant que moyen sans aiguille pour identifier et caractériser la cardiomyopathie ischémique chez les patients atteints l’IC.

5. THESIS OVERVIEW

This body of work consists of three chapters. Chapter 1 will define HF, its etiologies, and the current relevant methods of clinical investigation. Chapter 1 also serves to introduce OS-CMR and its potential for the noninvasive assessment of cardiomyopathy via standardized vasoactive breathing maneuvers. Chapter 2 will detail the methods and results of the study which investigates the capacity of OS-CMR paired with breathing maneuvers to differentiate ischemic from non-ischemic cardiomyopathy. Chapter 3 will provide discussions of the findings, limitations, and future directions.

Chapter 1: Introduction

An Introduction to Oxygen-Sensitive CMR For Assessing Heart Failure

Chapter 2: Original Research

Differentiation of Ischemic vs. Non-Ischemic Cardiomyopathy by OS-CMR

Chapter 3: Discussion and Conclusion

ICM vs NICM: Insights and future directions with OS-CMR

6. CONTRIBUTION OF AUTHORS

Dr. Matthias Friedrich is the Principial Investigator under which this study was completed. Dr. Friedrich also serves as leader of our research team, and as supervisor for this thesis.

Dr. Elizabeth Hillier (EH) served as the expert to whom I fielded questions about HF, OS-CMR, and their interactions. EH also served as secondary reader in the assessment of interobserver variability.

Furthermore, this investigation was also planned and executed with the guidance and assistance of Dr. Mitchel Benovoy and Dr. Judy Luu.

7. Chapter 1: An Introduction to Oxygen-Sensitive CMR For Assessing Heart Failure

Summary

Heart failure (HF) is a challenging and increasingly prevalent condition. Investigations to elucidate the etiology of HF is necessary for effective treatment. Currently, a comprehensive clinical strategy may involve diagnostic imaging techniques involving invasive procedures, ionizing radiation, pharmacological stress, and contrast agents. Oxygenation-Sensitive Cardiovascular Magnetic Resonance (OS-CMR) is a novel imaging technique which can assess dynamic changes in myocardial oxygenation without the aforementioned drawbacks to patient safety. Previous OS-CMR studies have established this technique as a valid methodology to identify abnormal oxygenation patterns in ischemic cardiomyopathy (ICM) and non-ischemic cardiomyopathy (NICM) compared to healthy patients. Furthermore, OS-CMR paired with a vasoactive breathing maneuver (Respiratory OS-CMR, ROS) provides a window into endothelial pathways of vascular function. ROS may serve as an effective way to differentiate ICM and NICM. ROS may provide insight into underlying pathophysiology, clinical workflow streamlining, and an improved prognosis in HF patients.

Introduction

HF is a chronic and progressive disorder in which the myocardium cannot expand and/or contract effectively, resulting in impaired filling and/or emptying of the cardiac chambers (1). At reduced efficiency, the heart cannot supply enough oxygen and nutrient-rich blood to meet the metabolic needs of the body. To accommodate for the deficiency, the heart may dilate, develop more muscle mass, increase contractility, and beat faster. Although these measures may compensate initially, the pathological processes underlying HF will continue to advance. Decompensated HF can manifest as a combination of fatigue, dyspnea, reduced exertional tolerance, and/or fluid retention (2). HF can severely increase morbidity of a patient and increase the risk of death. Despite considerable advances in prevention and intervention, mortality in HF patients remains as high as 75% at 5 years (3).

HF is a global issue affecting more than 64 million people (4). It is the leading cause of hospitalization among adults (4), and its prevalence is growing due to an ageing population (1,5,6). Consequently, the burden of HF-related hospitalizations and costs are also increasing. HF costs are currently estimated at US$30.7 billion, with an expected increase to $69.8 billion by 2030 (7). Without streamlining of clinical management, improved cost, and better therapeutic outcomes, HF will remain a worsening medical, societal, and economic problem (8).

Heart Failure

Ischemic and Non-Ischemic Etiologies

HF is a clinical syndrome rather than a specific disease with a defined pathophysiological mechanism. Optimal treatment and improved prognosis for a given case of HF requires thorough investigation of etiology. Cardiomyopathy broadly defines the group of heterogeneous structural and/or functional cardiac abnormalities that lead to HF (9). Cardiomyopathy can be divided into ischemic cardiomyopathy (ICM) and non-ischemic cardiomyopathy (NICM) (10).

ICM is defined by abnormal myocardial vasculature and resulting pathological changes in the dynamics of blood supply and tissue oxygenation. The majority of ICM is caused by the atherosclerotic processes leading to coronary artery disease (CAD) (11), but other notable sources of ICM include Ischemia with No Obstructive Coronary Arteries (INOCA), myocardial scarring, abnormal coronary microcirculation, and endothelial dysfunction. ICM is generally characterized by the pathomechanisms of myocardial ischemia which result initially in a reversible loss of cardiac contractile function. Prolonged ischemia, however, leads to irreversible myocardial damage and ensuing cardiac remodeling. Remodeling is primarily stimulated by myocardial fibrosis which causes decreased ventricular function, arrhythmia, and potential conduction system dysregulation (11).

NICM functions as a catch-all for causes of decreased heart function unrelated to myocardial ischemia. NICM includes infiltrative processes, metabolic derangements, genetic abnormalities, immune and inflammatory damage, toxicity-related damage, abnormal loading

conditions (hypertension, volume overload, cardiac structural defects and disease), and arrhythmias (12,13). Often, cases of NICM is described as dilated (stretched myocardium), hypertrophic (thickened myocardium), or restrictive (stiffened myocardium) cardiomyopathy, although these too can be caused by ischemic pathomechanisms (10,14).

Coronary Microvascular Dysfunction

In both NICM and ICM, coronary microvascular dysfunction (CMD) is evidenced as a fundamental pathophysiological factor, and is associated with worse prognosis and higher incidence of cardiovascular events (15–20). CMD is defined by abnormal function of the endothelium, a layer of cells in blood vessels which play a crucial regulatory role in coronary vascular function and thus cardiovascular homeostasis. The potential mechanisms of CMD are varied, including enhanced vasoconstrictive reactivity at the microvascular level, impaired endothelium-dependent and endothelial-independent microvascular vasodilation capacities, and increased microvascular resistance secondary to structural factors (21). CMD is a major contributor to many ICM and NICM conditions, in addition to hypertension, obesity, and diabetes (22,23) – all of which are significant risk factors for HF (24). Investigation of CMD in HF is not typical during clinical work-up or management, however, a growing body of evidence suggests that it is an important prognostic factor, especially in CAD and nonsignificant CAD (21).

Clinical Management

The treatment of HF entails a multifaceted approach involving patient education, pharmacological regimen to recover cardiac performance, and prevention of exacerbations (25). For patients presenting with a history and physical findings suggestive of HF, the first steps of diagnostic work-up are an assessment of left ventricular systolic function and identification of ICM or NICM as the underlying pathology (26).

Phenotypic characterization of HF by left ventricular ejection fraction (LVEF) facilitates risk stratification and guides therapy. A recent revision of HF classification guidelines defines four subcategories of HF based on LVEF: HF with reduced Ejection Fraction (LVEF ≤40%, HFrEF), HF with mildly reduced Ejection Fraction (LVEF 40-49%, HFmrEF), HF with improved Ejection

Fraction (LVEF ≤40% at baseline and a ≥10-point improvement on second measurement to an LVEF ≥40%, HFimpEF), and HF with preserved Ejection Fraction (LVEF ≥50%, HFpEF) (27).

Although the clinical presentation of ICM and NICM-derived HF may be indistinguishable from one another (28), the identification of either ICM or NICM as the pathological cause of HF is imperative for guiding treatment and prognosis (13,28–31). Notably, it is the investigation of possible ICM that leads this process.

ICM is the most common cause of HF (32). ICM develops when the heart's ability to pump blood is impaired due to the impedance of blood flow to the myocardium. The most prevalent form of ICM is CAD secondary to atherosclerosis, with approximately half of acute HF and half of HFrEF cases caused by CAD (33).) Ischemic etiology and, moreover, extent of CAD, is a significant independent predictor of mortality in patients with cardiomyopathy. ICM therapeutic strategies include revascularization, and antiplatelet and lipid lowering agents. Early revascularization, which is accomplished either by coronary artery bypass (CABG) surgery, angioplasty, and/or stenting, is strongly associated with better survival and its prioritization is of critical importance (28,34).

The investigation of possible NICM follows the exclusion of ICM. Due to the broad spectrum of NICM pathologies, the diagnostics and prognoses associated with NICM-mediated HF vary widely, as do management strategies, with pharmacological agents and device therapy often involved (12,35).

The goal of therapy for HF is to improve symptoms and quality of life, minimize hospitalizations, and reduce overall disease mortality. Innovation towards a reliable, noninvasive, streamlined, and cost-effective method of differentiation of ICM vs NICM-derived HF is vital for better therapy and outcomes for HF patients (27,36,37).

Utility of Diagnostic Imaging

Investigation of HF using cardiac imaging is standard. Transthoracic echocardiography is often the first-line imaging modality for HF. It is especially useful for early quantification of LVEF

(25). Echocardiography is more cost-effective than other common imaging modalities, widely available, relatively simple to operate, and can be used at bedside. However, image quality and the precision of measurements can be unreliable (27). Furthermore, echocardiography provides minimal information regarding myocardial tissue or coronary vascular function, and must often be supplemented by other imaging modalities to reach a comprehensive diagnosis (38).

The current clinical standards for identifying the presence of ICM and extent of myocardial ischemia (or excluding ICM and indicating an investigation of NICM by other means) are coronary angiography and fractional flow reserve (FFR), respectively. These are invasive processes that require cardiac catheterization, exposure to ionizing radiation, and intravenous administration of contrast agents. Catheterization alone carries complication rates estimated at 2% and is increasingly risky in patients with older age, renal insufficiency, uncontrolled diabetes mellitus, and morbid obesity (39). It is estimated that up to half of patients undergoing coronary angiography are found to have no obstructive CAD (40,41). Consequentially, a significant number of patients undergo an invasive procedure that rules out disease (CAD) but does not provide information on the existing underlying condition. Furthermore, many patients with overt symptoms of myocardial ischemia do not show significant obstructive coronary lesions via angiography, yet a substantial proportion of these patients are found to have CMD (42). Coronary angiography and FFR are not suitable to characterize ischemia not caused by an obstructed coronary artery (INOCA). Additionally, these techniques are not able to assess the spatial distribution or temporal dynamics of myocardial perfusion or oxygenation to identify CMD, which as mentioned previously is strongly associated with the development of HF (43).

Cardiac positron emission tomography (PET) and computed tomographic coronary angiography (CTCA) are two imaging modalities which allow for the comprehensive evaluation of spatial distribution of myocardial blood flow, and therefore the ability to differentiate ICM and CMD. However, their diagnostic utility is hindered by low spatial resolution, limited availability (PET) (44), ionizing radiation, and logistical challenges with tracers (45).

Cardiovascular magnetic resonance (CMR) is another imaging modality with significant utility in ICM and NICM. CMR-based late gadolinium enhancement (LGE) and first-pass

perfusion imaging are techniques capable of evaluating ischemic scar and spatial distribution of myocardial blood flow, respectively, with the drawback of requiring contrast and/or stress agents (46). The principles of magnetic resonance imaging, its current utility in HF, and emerging technologies in the field of CMR are detailed in the section that follows.

In light of the current mortality and morbidity rates, it is clear that there is room for improvement in medical strategies for HF. It is important to increase our understanding of HF pathophysiology and improve therapy for HF patients. An imaging modality which is non-invasive, free of ionizing radiation and contrast agents, and able to comprehensively differentiate and evaluate the underlying etiology of a patient with HF as ICM or NICM could be a significant advancement. Such an imaging tool could streamline clinical management, reduce the risk and cost of HF workup, and guide more informed therapy.

Cardiovascular Magnetic Resonance Imaging

Principles of Magnetic Resonance

Magnetic Resonance Imaging (MRI) functions based on the principles of nuclear magnetic resonance. MRI exploits the properties of hydrogen nuclei, which behave as small bipolar magnets. Usually oriented randomly, these nuclei will align in the direction of a magnetic field, like the one found inside an MRI machine. Put simply, changes in magnetic resonance signals as these nuclei are disrupted in their arrangement and then return to that arranged state can be collected and transformed into images (47). This disruption is accomplished by bursts of high energy radiofrequency (RF) pulses that push the nuclei in an excited state of resonance. Interruption of the RF pulse allows nuclei to return to their state of alignment in the magnetic field while simultaneously emitting an electromagnetic signal which is received by the MRI scanner hardware. This signal is spatially encoded and processed to produce an interpretable MRI image (48). Different tissues will produce different signal intensities, which allow clinicals to characterize anatomy and tissue and pathological abnormalities therein (49).

Utility of CMR in HF

Cardiovascular Magnetic Resonance (CMR) is the widely accepted gold standard for the qualitative and quantitative assessment of the heart, and a versatile diagnostic tool for the comprehensive investigation of HF etiology (50). CMR is routinely and increasingly used in the investigation of HF to aid in diagnosis, risk stratification, therapeutic guidance, and monitoring (50,51) as a result of its ability to provide detailed information on function, morphology, and myocardial tissue composition (52,53). Furthermore, studies have shown that compared to echocardiography, CMR provides more accurate measurements of function and tissue characterization (10), more accurately classifies HF patients into LVEF subgroups (54,55), and better establishes specific diagnoses within HFpEF (55,56), which comprise more than 50% of all HF patients (57).

Current clinical guidelines recommend the use of late gadolinium enhanced (LGE)-CMR in HF when echocardiography is non-diagnostic (13). LGE-CMR provides an accurate evaluation of myocardial scarring, however, it requires the use of gadolinium-based contrast agents. Administration of gadolinium-based pharmaceuticals causes discomfort and is not suitable for patients with renal failure or known contrast media allergy (58). Furthermore, LGE cannot identify or evaluate INOCA.

The clinical utility of first-pass perfusion stress CMR in suspected ischemic HF is also well established. In addition to being very accurate in the identification of ischemic myocardial tissue, stress CMR is associated with lower cost, and similar outcomes despite fewer angiographies and revascularizations compared to coronary angiography with FFR (59–61). Although free of ionizing radiation, CMR first-pass perfusion is, however, limited by its requirement for the injection of gadolinium-based contrast agents and pharmaceutical vasodilatory agents.

Oxygenation-Sensitive Cardiovascular Magnetic Resonance

Principles of OS-CMR

Blood hemoglobin can exist in either an oxygenated or deoxygenated state. Each state has a unique set of magnetic properties, the dynamics of which are exploited in MRI images sensitive

to the Blood-Oxygen-Level-Dependent (BOLD) effect (62). Oxyhemoglobin has no magnetic moment and does not significantly alter the measured magnetic field within the MRI machine. Deoxyhemoglobin, however, is paramagnetic which causes a disruption in the local magnetic field, and therefore an accelerated relaxation of surrounding protons (63). In BOLD images, as this disruption increases, the signal intensity decreases (64). Oxygenation-Sensitive CMR (OS-CMR) imaging is a non-invasive technique which can measure regional myocardial tissue oxygenation changes by means of the BOLD effect (65,66).

The balance of oxygen supply and demand in the myocardium is tightly regulated by a complex coupling of myocardial energetic processes and coronary blood flow. In the case of increased myocardial work and thus increased oxygen demand, a healthy coronary vasculature compensates by upregulating coronary blood flow through vasodilation (67). Due to the sensitivity of this homeostatic mechanism, the oxygenation status of the myocardium would be unaffected, and thus no change in the BOLD effect would be detected. Coronary vasodilation and an unchanged myocardial oxygen demand however, would result in a reduction of deoxyhemoglobin concentration, and an increase in signal intensity (68). Thus, in the context of OS-CMR, vasoactive [stress] interventions which alter blood volume, blood flow, or the balance of oxygen demand and supply in the myocardium can induce changes in hemoglobin oxygenation levels and create BOLD-sensitive images of the myocardium (68). The spatial and temporal dynamics of BOLD signal intensities therefor act as markers of coronary vascular function, endothelial dysfunction, and myocardial tissue oxygenation.

Endothelial Dependence in Induced Vasoactive Stress

Historically, a number of studies utilizing OS-CMR induced vasoactive stress using pharmacological agents such as adenosine that induce endothelium-independent vasodilation. In combination with adenosine, OS-CMR can be used for assessing myocardial perfusion and oxygenation in many disease states (28). Endothelium-independent vasodilation bypasses the endogenous regulatory mechanisms of the endothelium and acts directly on the vascular smooth muscle to cause vasorelaxation (69). As previously explained, such an intervention will decrease blood deoxyhemoglobin concentration and result in an increase in OS-CMR signal intensity in

healthy myocardium (70). Endothelium-independent vasodilation thus introduces hyperemic myocardial perfusion in healthy tissue which can be assessed by OS-CMR.

Although the endogenous contrast in OS-CMR eliminates the administration of gadolinium-based contrast agents, the use of pharmacological vasodilatory agents is still inconvenient and is not without risks (71). Furthermore, adenosine and analogues act solely through endothelium-independent vasodilation. The mechanisms underlying the natural microvascular response to increased myocardial oxygen demand, however, may be endothelium-independent and/or endothelium-dependent (72). Notably, CMD may be a functional characteristic of endothelial-independent and/or endothelial dependent vasodilation (73), as emphasized by the increased mortality risk found in HF patients who have endothelial-dependent dysfunction (20,74). Moreover, given the major prognostic role of endothelial-dependent dysfunction in both ICM and NICM (75,76), an assessment which includes endothelial-dependent mechanisms of vasodilation may serve as an important biomarker. More representative of physiological stress, a comprehensive assessment of endothelial-dependent and endothelial-independent function may therefore have a more significant prognostic value in HF and be more informative in terms of therapeutic consequences (77,78).

Standardized Vasoactive Breathing Maneuvers

Blood carbon dioxide (CO2) modulates endothelial-dependent vasoactive mechanisms in the coronary circulation (79). In response to hypercapnia, healthy coronary vasculature dilates and increases myocardial perfusion, a process similar to that observed during physiological stress (80). Hypocapnia on the other hand, induces coronary vasoconstriction and a reduction in perfusion.

Studies have found consistent and reproducible changes in signal intensity in OS-CMR performed with direct modulation of inhaled CO2 percentage (81,82). This approach, however, produces frequently intolerable side effects related to the urge to breathe and associated anxiety (83). By using respiratory maneuvers such as hyperventilation and breath-holding to manipulate blood CO2, OS-CMR can be performed without the need for inhaled gas modulation or additional equipment. In fact, in healthy populations (84,85), respiratory OS-CMR (ROS) has demonstrated

the potential for a more significant physiological stress response than adenosine OS-CMR, with less side effects (70).

A standardized respiratory maneuver which is comprised of 2 minutes of breathing at rest, followed by a 60-second period of paced deep breathing (hyperventilation) at 30 breaths-per-minute, and a subsequent breath-hold maintained for as long as is tolerable, has emerged as an effective mechanism of endothelial-dependent vasoactive stress (82,86). The resting period serves as a signal intensity baseline, while the hyperventilation induces coronary vasoconstriction, and the voluntary maximal breath-hold induces coronary vasodilation (87). During continuous OS-CMR image acquisition, the OS-CMR signal intensity difference between respiratory-modulated vasoconstriction and vasodilation is defined as the breathing-induced myocardial oxygenation reserve (B-MORE).

In summary, ROS assessment of B-MORE exists as a safe, fast, non-invasive, and convenient tool that avoids the use of needles, exogenous contrast agents, harmful radiation, or specialized additional equipment. In the investigation of ICM vs NICM-derived HF, OS-CMR B-MORE offers not only a fully quantitative assessment of cardiac morphology, function, and tissue characteristics, but also high-resolution information on endothelial dysfunction (CMD). OS-CMR has the potential to improve the management of HF patients and to introduce novel imaging biomarkers that may advance risk stratification as well as our understanding of HF pathophysiology.

Utility in Ischemic and Non-ischemic Etiologies of HF

Previous research has confirmed that OS-CMR B-MORE can identify healthy myocardium, ICM, and NICM by analysis of global and regional BOLD signal intensity (SI) dynamics. Specifically, in comparison to age-matched healthy subjects, ICM (88) and NICM (89) patients had respectively unique and significantly attenuated regional myocardial oxygenation responses to breathing maneuvers.

In animals and CAD patients, OS-CMR B-MORE has detected patterns of reduced myocardial perfusion and oxygenation in myocardial territories subtended by an angiographically

significant coronary artery stenosis (87,88). Furthermore, adenosine OS-CMR has accurately detected myocardial oxygenation deficits downstream of both flow-limiting (62,90) and non-flow limiting (91–93) coronary artery stenosis, indicating that perfusion deficits alone do not always indicate underlying oxygenation deficits. This becomes particularly important when considering recent studies that compared medical therapy to procedural intervention (i.e. revascularization) as a first-line clinical management in HF and found no significant differences in patient clinical outcomes (61,94). The dissociation between myocardial perfusion and oxygenation may be an important component in the pathophysiology of HF. An understanding of their independent and interdependent roles in disease mechanism, risk profile, and patient outcomes may impact therapeutic strategies in HF.

In patients with INOCA, half of which have been estimated to have CMD (95), OS-CMR B-MORE identified regional myocardial oxygenation deficits. Suggestive of a potential role of endothelium-dependent CMD (89), these findings are consistent with previous studies that showed evidence for heterogeneity of microvascular function (96). The dysfunctional myocardial oxygenation response in these populations reflects our current understanding of the involvement of endothelial dysfunction.

OS-CMR-based examination of myocardial oxygenation and thus microvascular disease states have enhanced the investigation of underlying pathophysiology in patients with ICM, and has also further elucidated the role of CMD in NICM. A reduced B-MORE and thus indication of coronary microvascular dysfunction has been demonstrated in patients with obstructive sleep apnea, heart transplantation, and aortic stenosis (97–99). Studies with adenosine OS-CMR have found impaired myocardial perfusion and oxygenation in non-ischemic dilated cardiomyopathy and hypertrophic cardiomyopathy populations (100,101). The impaired myocardial oxygenation response observed in these NICM populations reflects our current understanding of endothelial dysfunction in these populations (99).

Limitations of OS-CMR

CMR and OS-CMR are both limited by a lack of access to MRI scanners, local expertise, high cost, and scan contraindications such as claustrophobia (102). Requiring no contrast agents, specialized equipment, or the presence of a trained physician, OS-CMR combined with breathing maneuvers may mitigate some of the issues CMR has historically faced. However, this technique does require local expertise for the training of breathing maneuvers, and specific software to analyze oxygenation dynamics, the latter of which may be costly to develop and purchase.

There are several other limitations specific to OS-CMR that must be explored further and addressed in future works.

MRI scanner field strength is an important consideration. MR signal sensitivity to deoxygenated hemoglobin is decreased and therefore limited at 1.5T (Friedrich and Karamitsos, 2013). At 3T, the signal-to-noise ratio is increased and thus the contrast between oxygenated and deoxygenated myocardium is more pronounced (Dharmakumar et al., 2008). However, artifacts are more common at higher field strengths. Although these can be somewhat mitigated by precise shimming in the operation of the MR, artifacts can impact the clinical interpretability of OS-CMR images (Friedrich and Karamitsos, 2013).

OS-CMR measurements of oxygenation changes are also sensitive to physiological variables. OS-CMR signal intensity is sensitive to blood flow, blood oxygenation saturation, as well as blood hematocrit levels (Vohringer et al., 2010, Guensch et al., 2016). As such, absolute signal intensity values may vary between subjects and within subjects depending on factors such as hydration status and altitude adaptations (Guensch et al., 2016, Akunov et al., 2018, Leon-Valarde et al., 2000).

Lastly, no standard reference values exist yet to denote OS-CMR signals and B-MORE ranges as healthy or pathological. Additionally, reader bias may affect analysis as current methods in OS-CMR require manual segmentation and analysis of OS-CMR images. As such, current values can only be compared within the site they've been acquired from, and human error must be considered as a factor in the analysis and interpretation of results.

Conclusion

Despite considerable advances in prevention and intervention, mortality and morbidity for HF patients remain high and quality of life poor (103). Identifying the cause of HF as either ICM or NICM is an early clinical step in HF management that has important prognostic and therapeutic implications. For HF, CMR is the most comprehensive and accurate diagnostic tool. OS-CMR imaging paired with a breathing maneuver (ROS) is a needle- and contrast-free technique which examines the dynamic conditions of myocardial oxygen supply and demand in the heart. This OS-CMR technique may further advance clinical decision-making by providing novel insights into the pathophysiology of ICM in HF patients. OS-CMR has already demonstrated its clinical utility in multiple studies of patients with various cardiac diseases associated with HF, including ICM, NICM, arterial hypertension, and patients with microvascular dysfunction in the absence of CAD. Previous research has confirmed that OS-CMR B-MORE can identify healthy myocardium, CAD, and contribute towards the pathophysiological understanding of NICM. Notably, OS-CMR B-MORE may have the capacity to differentiate ischemic from non-ischemic etiologies of HF by identifying and characterizing dynamics of global and regional dynamics of myocardial oxygenation. Importantly, the use of breathing maneuvers via ROS will assess endothelium-dependent and endothelium-independent coronary function which may increase the diagnostic power of OS-CMR B-MORE compared to contrast- and pharmacological-dependent imaging methods.

8. CHAPTER 2: ORIGINAL RESEARCH

Methods

The aim of Differentiation of Ischemic versus Non-ischemic cardiomyopathy by OS-CMR (DINO) is to assess the ability of breathing-induced OS-CMR biomarkers to differentiate cardiomyopathy as ischemic or non-ischemic. DINO may offer a deeper understanding of ICM and NICM pathophysiology, and thus insight and direction towards improved management and prognosis in the HF population.

Study Design

This is a retrospective, cross-sectional cohort study. OS-CMR data was obtained from study data at the McGill University Health Centre (MUHC) in Montreal, Canada. Study data originated from patients enrolled in the prospective clinical trial approved by the appropriate local ethics boards: *A 10-Minute Cardiovascular Magnetic Resonance Protocol for Cardiac Disease* (#2020-6128) between November 2019 and April 2022.

Participants

Participant inclusion criteria included subject age above 18, informed consent, and a diagnosis of ICM or NICM as per the clinical report. Exclusion criteria were general MRI contraindications, recent consumption of caffeine or vasoactive medications, inability to complete the breathing maneuver, unstable hemodynamics, and problematic arrhythmia (Table 1).

Table 1: Inclusion and Exclusion Criteria

Criteria	ICM Group	NICM group	All
Inclusion	• Diagnosis of ICM by CMR and/or angiography, clinical report used as standard of reference. See table 3 for list of diagnoses.	• Diagnosis of NICM by CMR, clinical report used as standard of reference. See table 3 for list of diagnoses.	• Age > 18 y • Informed consent
Exclusion	• General MRI contraindications including MR-incompatible pacemakers, intracranial aneurysm clips, metallic foreign bodies, and pregnancy. • Consumption of caffeine or vasoactive medications 12 hours before the CMR exam. • Unable to complete breathing maneuvers. • Hemodynamically unstable condition • Significant/uncontrolled arrhythmia		

Initially, 44 patients including 26 subjects with ICM and 18 subjects with NICM were identified for inclusion in the study.

Clinical Variables

All patients had a CMR exam including standard function, mapping, and OS-CMR paired with a standardized breathing maneuver. The data used in this study included global and segmental signal intensity values measured during the BH portion of OS-CMR image acquisition, in addition to demographic characteristics from study records (body mass index (BMI), body surface area (BSA), age, sex, weight, height, vital signs, and health status) documented at the time of the clinical scan.

CMR Protocol

MRI imaging of the heart was performed using two clinical MRI scanners of 3.0 Tesla: SIGNA Premier, GE Healthcare (Chicago IL), and MAGNETOM Skyra, Siemens Medical Solutions (Erlangen, Germany).

Participants were asked to refrain from consuming caffeine or taking beta-blockers for 12 hours leading up to the exam. All study subjects underwent the same ROS scanning protocol. The

ROS imaging protocol involved a baseline OS-CMR acquisition, followed by 60s of hyperventilation (metronome-paced at 30 breaths/min), and then by a voluntary maximal breath-hold, during which OS-CMR images were acquired continuously in basal and mid-ventricular short-axis slices. Subjects were coached through and practiced the breathing maneuvers before the scan. The participants were continuously monitored for any adverse effects. A detailed description of the OS-CMR sequence and parameters has been described in detail (84,88,104).

CMR Image Blinding and Analysis

OS-CMR images were anonymized using a primary code and assigned a secondary code to blind readers from participant identities. The first reader, SC, analyzed all de-identified OS-CMR images using cvi42 (Circle Cardiovascular Imaging, Calgary, Canada) software. cvi42 was used to identify scans with poor image quality and/or incomplete breathing maneuvers for exclusion, demarcate the BH portion OS-CMR image acquisition and adjust the semi-automatic contouring of the epicardium and endocardium (88). The first and last images of the breath-hold closest to 0s and 30s, respectively, were of the end-systolic portion of the cardiac cycle. Epicardial and endocardial semi-automated contours were offset to the interior by 10% to avoid partial volume effects. A second independent reader with significant experience, EH, performed the same analysis in 20% of the participants to control for biases in analysis technique.

OS-CMR image data was reported using global and segmental values in accordance with the American Heart Association's (AHA) standardized model of myocardial segmentation (105). All signal intensity values were normalized using the highest and lowest values measured in the myocardium throughout the BH automatically within cvi42 software.

Additional patient data retrieved included heart rate data, resting systolic/diastolic blood pressures, hemodynamic data, patient demographics and characteristics data. Numerical and categorical (non-identifying) demographic information: gender, BMI, height, weight, BSA, age.

Statistical Analysis

Statistical analysis was performed using GraphPad Prism version 9.0.0 for Mac OS (GraphPad Software, San Diego, California USA, www.graphpad.com). BMI and BSA were

calculated from patient height and weight via the Mosteller formula: BMI = kg/m2, BSA = sqrt(kg*cm/3600).

Measurements of global and regional oxygenation dynamics used for statistical analysis were determined from the first post-hyperventilation BH end-systolic image, and the end-systolic image closest to 30 seconds of the breath-hold (Figure 1). This study analyzed ROS SI data using normalized values.

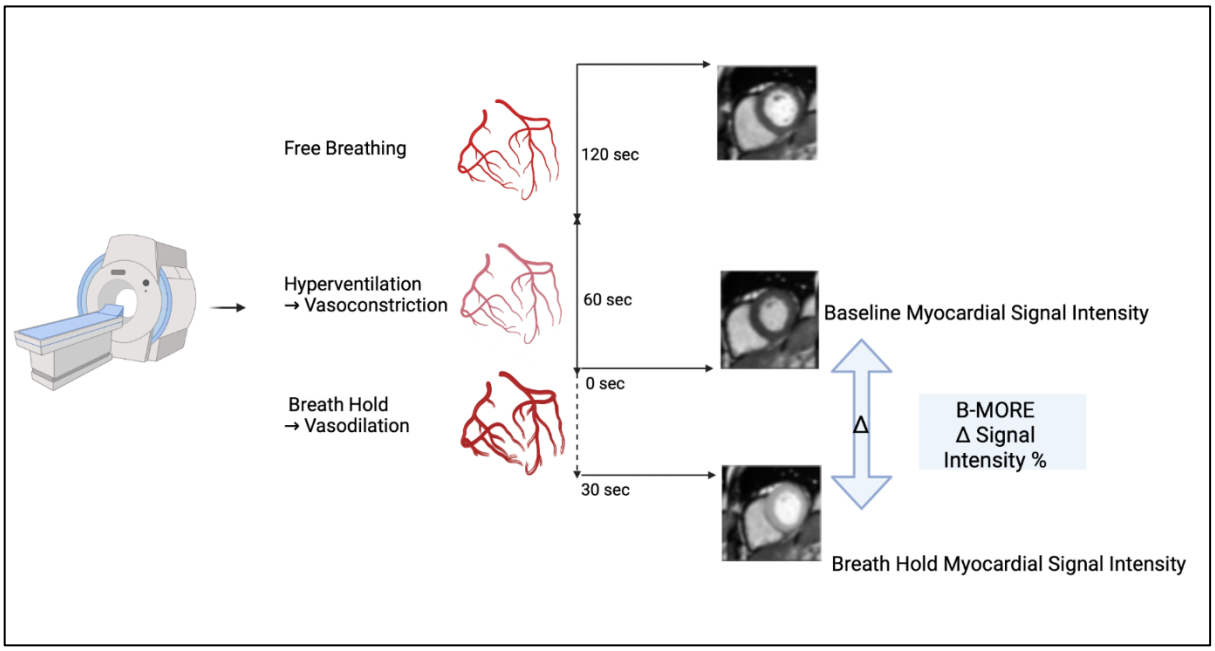

Figure 1: Myocardial oxygenation is assessed between the signal intensity of the first post-hyperventilation end-systolic image (at end of hypocapnia-induced vasoconstriction), and the signal intensity of the end-systolic image closest to 30 seconds into the BH, (during hypercapnia-induced vasodilation). Image produced using Biorender.com, courtesy of Kate Lindsay.

Global metrics refer to an inclusion of all AHA segments, whereas regional metrics refer to an inclusion of singular AHA segments or the sum of AHA segments that make up the coronary territories. Segments refer to basal (1-6) and mid (7-12) segments of the 17-segment model for segmentation of the LV as presented by the AHA (105). For the purposes of statistical analysis,

the coronary territories refer to the combination of basal and mid segments as the apical slice was not part of OS-CMR acquisition: LAD (1,2,7,8), RCA (3,4,9,10), and LCX (5,6,11,12) (Figure 2).

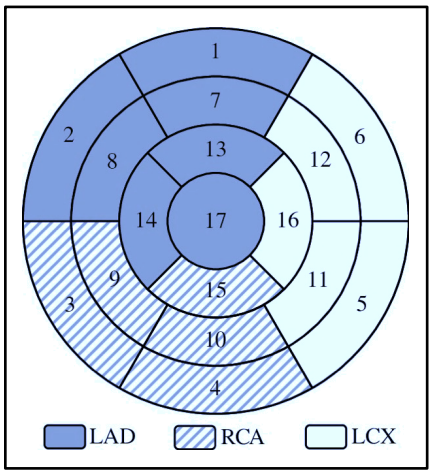

Figure 2: The 17-segment model for the segmentation of the LV as presented by the AHA. The patterns indicate the mapping of the segments to coronary territories (106).

The following biomarkers were produced from SI values between the first and last end-systolic images (inclusive) of the first 30 seconds of the post-hyperventilation BH (Figure 1). Percent SI change (ΔSI%) across the BH is an established biomarker which was employed as an endpoint in many of the referenced OS-CMR studies (84,88,97,99,101). Other ΔSI biomarkers employed in this study were exploratory. Measures of standard deviation (SD) were assessed as an exploratory surrogate markers for oxygenation (vascular response) homogeneity across the BH, which was recently explored in a study of INOCA and shown to be significantly decreased in female patients with INOCA compared to healthy controls (89). Further explanation of these experimental biomarkers is detailed in the discussion section.

Global:

1) ΔSI% across the BH (difference between SI in end-systolic image at 0s and 30s).
2) Slope of the average global SI across the BH (includes all images from 0s -30s). This slope is calculated from the line of best fit.
3) SD of global SI across the BH (includes all images from 0s -30s)

4) Slope of global SD of global SI across the BH (includes all images from 0s -30s). This slope is calculated from the line of best fit.

Regional:

1) Minimum segment ΔSI across the BH (difference between end-systolic SI in image at 0s and 30s).
2) Range of segment ΔSI (maximum segment ΔSI – minimum segment ΔSI) across the BH (difference between SI in end-systolic image at 0s and 30s).
3) Minimum coronary territory ΔSI across the BH (difference between end-systolic SI in image at 0s and 30s).
4) Range of coronary territory ΔSI (maximum coronary territory ΔSI – minimum coronary territory ΔSI, difference between SI in end-systolic image at 0s and 30s).

A two-tailed, unpaired homoscedastic (equal variance) Student's t-test was performed on all metrics across groups to assess the significance of differences in values between ICM and NICM.

A receiver operating characteristic (ROC) was performed on all metrics across groups to assess the diagnostic performance of each metric. The clinical report was used as the reference standard. In ROC analysis, an area under the curve (AUC) of 0.5 suggests no ability to discriminate ICM vs NICM based on the test, 0.7 to 0.8 is considered acceptable, 0.8 to 0.9 excellent, and above 0.9 outstanding (107).

A chi-square statistic was performed on select metrics categorized as binomials for positive or negative values.

A simple logistic regression model with a binary outcome of ICM and NICM was performed on all metrics. The clinical report was used as the reference standard.

A probability value (p) less than 0.05 was deemed significant. A Bonferroni correction was applied retrospectively to provide additional statistical perspective.

To determine intraobserver variability, intraclass correlation coefficient (ICC) analysis was performed on a randomly selected subgroup of 15 subject images analyzed twice by the primary reader, SC. To determine interobserver variability, analysis was performed on a randomly selected subgroup of 20 subject analyzed images analyzed both by SC in addition to an experienced CMR reader, EH.

Results

Study Population

Of the initially selected subjects, 12 were eliminated from the analysis due to incomplete breathing maneuvers and a resulting lack of data, which was only identifiable upon image analysis. Ultimately, the data of 33 individuals, 20 with ICM and 13 with NICM, was used in the final analysis. The baseline characteristics of all 33 analyzed subjects are summarized in Table 2. The study population had a mean age of 61.0 years (SD 15.7). The population was largely male (81.8%). There were no demographic characteristics that showed significant difference ($p<0.05$) across the ICM and NICM groups. Of the functional LV parameters measured by CMR (Table 2), there were no significant differences between the ICM and NICM cohorts. The specific condition of each patient is listed in Table 3.

Intraobserver and Interobserver Variability

The intraobserver variability of the B-MORE measurements was small. Assessed on a subgroup of 15 subject images read twice by SC, the ICC was 0.92, indicating excellent intra-observer reliability (108). The interobserver variability was also small, as assessed on a subgroup of 20 subject images read by two readers. For all slices, ICC results were above 0.82, and for global values, the ICC was above 0.81, indicating good reliability between readers for both metrics (108).

Global Myocardial Oxygenation Changes

The overall mean ΔSI% over the BH (B-MORE) across all subjects was 4.59 (95% confidence interval (CI) 0.7, 8.48). Though not statistically significant in a t-test ($p=0.241$), mean B-MORE was decreased in ICM at 2.69 (CI -3.33, 8.71) compared to 7.51 in NICM (CI 4.44,

10.58) (Figure 3A). When treated as a binomial for either positive change or negative change in global SI, ICM showed negative changes in 10 (50%) subjects, while NICM showed negative changes in 1 (8%) subject (Figure 3A). This difference was significant in a chi-square statistic (p=0.019). In ROC analysis, AUC was 0.696 (CI 0.511, 0.882), p=0.060 (Figure 3B).

The overall mean slope of the average global SI across the BH across all subjects was 0.08 (CI 0.02, 0.13). Note that this slope and the slope for global SD are calculated from the line of best fit to include all images across the BH (and not from the first and last images as done in ΔSI%). This value was not significantly different (p>0.5) between ICM (0.07; CI 0.00, 0.14) and NICM (0.09; CI -0.01, 0.19) (Figure 4A). Assessment of this metric as a positive or negative binomial yielded no significant difference between ICM and NICM in a chi-square statistic (p>0.5) (Figure 4A). In ROC analysis, AUC was 0.5423 (CI 0.337, 0.748), p>0.5 (Figure 4B).

The overall mean of global SD across the BH across all subjects was 4.48 (CI 4.05, 4.91). The value was not significantly different between (p=0.188) between ICM (4.23; CI 3.85, 4.62) and NICM (4.84; CI 3.94, 5.73) (Figure 5A). In ROC analysis, AUC was 0.5830 (CI 0.3660, 0.8000), p=0.431 (Figure 5B). One statistically significant outlier was excluded from this analysis (ICM; 9.43).

The overall mean slope of global SD across the BH across all subjects was -0.02 (CI -0.05, 0.01). This value was not significantly different (p=0.189) between ICM (0.00; CI -0.04, 0.04) and NICM (-0.04; CI -0.09, 0.01) (Figure 6A). Assessment of this metric as a binomial yielded no significant difference in a chi-square statistic (p>0.5). In ROC analysis, AUC was 0.687 (CI 0.484, 0.889), p=0.074) (Figure 6B).

Regional Myocardial Oxygenation Changes

The overall mean of minimum segment change across all subjects was -8.30 (CI -11.28, -5.33). The mean values in ICM (-10.10, CI -14.41, -5.79) were decreased compared to NICM (-5.55, CI -8.8, -2.3) (Figure 7A). This difference was notable but not statistically significant with p=0.145. In ROC analysis, AUC was 0.6308 (CI 0.4395, 0.8220), p=0.210 (Figure 7B).

The overall mean of the range of segment change across all subjects was 20.58 (CI 17.8, 23.37). The mean values in ICM and NICM were 19.84 (CI 17.87, 27.57) and 21.09 (CI 17.34, 24.84), respectively (Figure 8A), This difference was not statistically significant ($p>0.5$). In ROC analysis, AUC was 0.5425 (CI 0.3329, 0.7521), $p>0.5$ (Figure 8B). One statistically significant outlier was excluded from this analysis (ICM; 53.71).

The overall mean of minimum coronary territory change across all subjects was -4.68 (CI -13.15, 3.79). The mean values were decreased in in ICM (-10.57; CI -23.17, 2.04) compared to NICM (4.38; CI -3.06, 11.81) (Figure 9A). This difference was notable but not statistically significant with $p=0.091$. When treated as a binomial for either positive change or negative change, ICM showed negative changes in 14 (70%) subjects, while NICM showed negative changes in 4 (31%) subjects. This difference was significant in a chi-square statistic ($p= 0.027$). In ROC analysis, AUC was 0.692 (CI 0.508, 0.877), $p=0.065$ (Figure 9B).

The overall mean of the range of coronary territory change across all subjects was 20.81 (CI 18.2, 23.42). The mean values were increased in ICM (22.49; CI 19.89, 25.09) compared to NICM (18.49; CI 13.45, 23.54), respectively (Figure 10A). This difference was notable but not statistically significant $p=0.155$. In ROC analysis, AUC was 0.6154 (CI 0.3959, 0.8349), $p=0.280$ (Figure 10B). Two statistically significant outliers were excluded from this analysis (ICM; 85.6, 66.47).

Multivariable Analysis

In simple logistic regression analyses using a binary outcome of ICM or NICM, no individual biomarker achieved significance ($p<0.05$) (Table 4). Given that no biomarker achieved significance in univariable analysis, multivariable analysis was not performed.

9. CHAPTER 3: ICM VS NICM: INSIGHTS AND FUTURE DIRECTIONS WITH OS-CMR

Discussion

Summary of Results

Identifying the cause of HF as either ICM or NICM is an early clinical step in HF management that has important prognostic and therapeutic implications. OS-CMR imaging paired with a breathing maneuver is a needle- and contrast-free technique which examines the endothelium-dependent and endothelium-independent vascular function in the heart. OS-CMR B-MORE may have the capacity to differentiate ischemic from non-ischemic etiologies of HF by identifying and characterizing patterns of global and regional myocardial oxygenation.

In this novel study, we retrospectively assessed myocardial oxygenation patterns in ICM and NICM patients. While previous OS-CMR studies have differentiated between ICM and healthy patients (88,89), and NICM and healthy patients (100,101) this was the first study to investigate the differentiability of ICM from NICM. Furthermore, to our knowledge this was also the first study to use normalized SI values, as well as the first to investigate parameters of SI slope, SD slope, minimum segment B-MORE, segment B-MORE range, minimum coronary territory B-MORE, and coronary territory B-MORE range across the BH. Although few statistically significant differences across metrics were identified between the ICM and NICM cohorts, there were notable differences that would likely reach statistical significance given a larger sample size.

Given the exploratory nature of this study, numerous novel biomarkers were investigated. The statistical likelihood of a significant finding being false correlates positively with the number of findings. The Bonferroni correction divides the original alpha (set to 0.05) for controlling type 1 errors by the number of tests performed. In this case, there are 18 tests, and the Bonferroni correction would suggest that a statistically significant finding would be one with $p<0.00278$.

Global Variability in Myocardial Oxygenation

In related works with ROS, an impaired global ΔSI% (B-MORE) has been observed in ICM subjects (multivessel CAD) compared to healthy subjects (88,89). In a previous OS-CMR

study of female INOCA patients and healthy female participants, there was no significant difference in B-MORE between groups. However, there was a significant increase in regional heterogeneity of myocardial oxygenation in INOCA compared to healthy participants (89). An impaired B-MORE has also been observed in cardiac transplant patients (even in the absence of cardiac allograft vasculopathy) (97) and obstructive sleep apnea patients (99). These findings suggest that global B-MORE is sensitive to ICM in the presence of a significant perfusion deficit (existing CAD), but not when the underlying cause of ICM is CMD as hypothesized in INOCA (89). Yet, in the studies of cardiac transplant patients and obstructive sleep apnea patients, where no coronary obstruction exists, CMD is hypothesized as the mechanism of impaired B-MORE (97,99).

Beyond the inconsistency in previous findings, a notable limitation of global B-MORE is that its calculation relies exclusively on the first and last images of the BH. We hypothesized that global biomarkers assessing SI dynamics that use all images collected throughout the BH may be more sensitive to impaired myocardial oxygenation in ICM that would differentiate it from NICM in a HF population. We believe that an enhanced sensitivity is of particular importance given that CMD is prevalent in ICM and NICM populations (15–20).

In our study mean ΔSI% (global B-MORE) was decreased in ICM (2.69) compared to NICM (7.51) ($p=0.241$). In ROC analysis, AUC neared the acceptable range at 0.696 ($p=0.06$). When classified as a binomial for negative or positive change, ICM showed negative changes in 10 (50%) subjects, while NICM showed negative changes in only 1 (8%) subject. This difference was significant in a chi-square statistic ($p=0.019$). In our study, global B-MORE appears to have clinical value in the differentiation of ICM and NICM. In particular, a negative ΔSI% may be an effective marker to indicate ICM. A prospective study involving an expanded sample size would better explore this question.

The other global biomarkers we investigated have not been explored in previous OS-CMR studies. As explained, their calculation included all images in the BH portion of the breathing maneuver as opposed to ΔSI% which only included the first and last images. Slope of the global SI trend, in particular, was investigated as an alternative to ΔSI%. This biomarker did not prove

more effective than ΔSI%. We found no significant difference between ICM and NICM mean values (0.07 and 0.009, respectively, p>0.5), little utility in conversion to binomial values (chi-square statistic p>0.5), and a lower and less significant AUC 0.54 (p>0.5). We suspect that this biomarker proved insufficient because it modeled the SI trend as linear and was therefore less sensitive to an increasing rate of SI change compared to ΔSI%.

Global SD across the BH was assessed as a marker of heterogeneity in myocardial oxygenation. Heterogeneity was previously demonstrated to be significantly increased in female INOCA patients compared to healthy subjects (89), however, our ICM group contained no INOCA patients, only CAD patients and patients with myocardial scarring. Given the pathophysiology of these conditions, we expected ICM to have less heterogeneity in myocardial oxygenation values compared to NICM as under-perfused or scarred regions would have a blunted vascular response and therefore occupy a smaller range of values. We found that mean SD was decreased in ICM (4.23) compared to NICM (4.84) (p=0.188). This finding suggests that if our cohort of ICM patients included representation for INOCA patients, Global SD mean would increase in the ICM group and thus further narrow the gap between mean ICM and NICM values. A larger study with ICM and NICM cohorts that better represent the breakdown and frequency of ICM and NICM conditions would serve to clarify this prediction.

Global SD slope across the BH was assessed as marker of dynamic heterogeneity in myocardial oxygenation. In healthy myocardium, blood flow increases approximately linearly with oxygen demand. At higher rates of myocardial blood flow, (MBF) efficient oxygen extraction depends on a corresponding decrease in capillary transit time heterogeneity (CTTH) (109). Altered capillary morphology in the setting of microvascular dysfunction may therefore manifest as a limited ability to reduce CTTH as MBF increases. An impaired capacity to decrease CTTH in response to increased MBF has been proposed as a mechanism for ischemia in CAD and INOCA (109). Theoretically in a healthy individual, as MBF increased across the BH, we would expect OS-CMR SI SD to decrease to reflect a similar trend in oxygenation and its relationship with CTTH. In our study, we expected the presence of impaired CTTH in ICM to manifest as an increased slope of SD across the BH compared to NICM. In our analysis, slope was mildly increased in the ICM (0.00 vs -0.04, p=0.189) group, however this difference was not statistically

significant. AUC in ROC analysis neared the acceptable range at 0.687 (p=0.074). Of note, this observation may not be reflective of CTTH for two reasons. First, we are assessing the SD between the SI of each segment, and not the SI of individual pixels. We may therefore lack the resolution to assess this phenomenon. Second, we expect that the regional nature of ischemic and scarred myocardium, and its impaired ability to oxygenate compared to remote myocardium, would itself contribute to in an increased rate of SD change across the BH in ICM compared to NICM.

Regional Variability in Myocardial Oxygenation

In previous OS-CMR studies of CAD, significantly attenuated BOLD SI changes have been measured in myocardial regions with perfusion deficits (90,110). In alignment with these findings, we expected patterns of abnormal myocardial oxygenation resulting from scarring or CAD in ICM to be localized, whereas in NICM, although pathological myocardial oxygenation has been observed previously, we expected it to be more diffuse.

A regional pattern of ischemia was expected to be identifiable by isolating segments and coronary territories with the least ΔSI across the BH. Isolation of the segment with the least ΔSI served as a parameter that would root out the most extreme myocardial oxygenation deficit, while isolation of the coronary territory with the least ΔSI would serve as a more powerful method to root out the consequence of a compromised coronary artery.

Minimum segment ΔSI was decreased in ICM (-8.30) compared to NICM (-5.55). Minimum coronary territory ΔSI was markedly decreased in ICM (-10.57) compared to NICM (4.38). As a binomial, this biomarker showed a difference between ICM and NICM that was significant in a chi-square statistic (p= 0.027). We believe these biomarkers to be of merit, as they may aid in the automation of CAD detection via OS-CMR. Further study is necessary.

We inspected the range of segment and coronary territory ΔSI from a similar angle of understanding. We hypothesized that ICM would have a larger range of ΔSI across regions compared to NICM due to blunted vascular dynamics of ischemic regions of myocardium. Range, as opposed to minimums, we thought might help us further differentiate diffuse vs localized dysfunction. Range of ΔSI across segments was decreased in ICM (19.83) compared to NICM

(21.09) (p>0.5), AUC 0.54 (p>0.5). When segments were combined into their corresponding coronary territories, ΔSI range across coronary territories was increased in ICM (22.49) compared to NICM (18.49) (p=0.155), AUC 0.62 (p=0.280). These results suggest that range of coronary territory ΔSI may be a more powerful indicator of ICM than range of segment territory ΔSI. Use of biomarkers that assess coronary territory, however, may not be sensitive to ICM not stemming from CAD.

Limitations

A number of limitations exist in this study. The first is sample size. We identified and included all available subjects retrospectively which fit the criteria of the study from the prospective trial, *A 10-Minute Cardiovascular Magnetic Resonance Protocol for Cardiac Disease* (#2020-6128) between November 2019 and April 2022. The inclusion criteria for this trial were age >18, informed consent, and a clinically indicated CMR exam. Exclusion criteria for this study reflect that of DINO. Of the approximate 700 patients included in the prospective trial, 44 subjects had either ICM or NICM in addition to an OS-CMR scan. Of these 44 subjects, 26 had ICM and 18 had NICM. During image analysis, 12 subjects were excluded due to variables not accessible prior to image analysis. Specifically, these subjects were excluded due to incomplete breathing maneuvers (<30s) or poor image quality, and a resulting lack of data. The nature of these exclusions may have resulted in a selection bias for more functional patients capable of performing the breathing maneuver correctly. Of the remaining 33 subjects, 20 had ICM and 13 had NICM. This sample size may have lacked the power to establish statistical significance in many of the differences we observed between groups.

Not all forms of ICM and NICM were represented in this study (Table 3). The clinical report diagnosed ICM patients with an inducible perfusion deficit (CAD) (15), and ischemic scar (5). NICM patients were diagnosed with either fibrosis (1), hypertrophy (7), infiltration (1), inflammation (2), noncompaction (1), and restrictive (1) disorders. Consequently, the findings of DINO cannot be applied to the entire populations ICM and NICM. We suggest a much larger prospective study to control for the variability in ICM and NICM conditions.

Risk factors were self-reported and as such unknown risk factors may exist within the cohorts. The participants of this study were predominantly male, and therefore it cannot be stated that similar observations would be made in females. Other factors could have contributed to altered SI values in this study including environmental factors (pollution), socioeconomic factors (income, education level), and/or physiological factors (hematocrit, coronary blood flow). Additionally, subject medication information was not available in this study beyond the source studies restriction for consumption of caffeine or vasoactive medications 12 hours before the CMR exam. Furthermore, although some level of quality control is present during analysis, the quality of the breathing maneuvers cannot be guaranteed to be identical across all patients. Future studies should be prospective in nature and assess and control for a wider range of factors in the to ensure the collection of reliable and informative data.

In this study, we chose to group all ischemic cardiomyopathy together, which meant grouping patients experiencing an acute myocardial perfusion deficit with patients with previous perfusion deficits. We did not exclude patients that had a previous myocardial infarction or patients who had undergone coronary artery bypass graft surgery. We expect that patients with scarring from previous ischemic events would produce different ROS SI data than patients with a current perfusion deficit. This distinction is important clinically, as patients with a known ischemic scar would be unlikely to undergo catheterization. In an expansion of this study, we would expect to have increased power and the ability to run multivariable analyses to investigate combinations of biomarkers which may be more robust in the differentiation of ICM and NICM.

Conclusions and Future Directions

As a one-stop, needle-free method for the differentiation of ICM vs NICM, ROS could improve the management and prognosis of the HF patient population. In the context of HF, ROS could be advantageous over current practices for several reasons. Unlike coronary angiography, FFR, PET, CTCA, and CMR LGE and first-pass perfusion, ROS is completely non-invasive; it does not require needles, contrast, or ionizing radiation. Second, CMR is the most comprehensive diagnostic tool for cardiovascular disease. CMR and ROS could streamline the diagnostic workup of HF patients, which may prove more clinically efficient and cost-effective than combining

echocardiography, coronary angiography, and PET to assess LV function, coronary obstruction, and myocardial perfusion, respectively. Lastly, ROS may identify and assess ICM caused by pathomechanisms of both endothelial-dependent and endothelial-independent CMD, an ability unique to this imaging technique.

This study investigated the capacity of ROS to distinguish between ICM and NICM through established and novel metrics of patterns of regional and global myocardial oxygenation. Given the small sample size of this study, it is unsurprising that no metric demonstrated a statistically significant difference via Student's t-test in ICM vs NICM. Nonetheless we did discover some metrics which appear promising and worthy of further study. These include global ΔSI% and minimum coronary territory SI change across the BH assessed as a binomial for positive or negative change, as well and global SD slope. There are additional biomarkers not investigated in this effort that would be of interest in a future study. These include intramural gradients of dysfunction toward the subendocardium, as has been observed recently in INOCA (104), and pixel-based SD as a high-resolution marker of heterogeneity and CTTH dynamics. We believe these biomarkers would be helpful in the detection of non-CAD ICM.

In a future investigation, we would execute a prospective study to avoid unforeseen loss of data and associated loss of power. We would employ a larger sample size of sex-balanced cohorts and improved representation for the spectrum of ICM and NICM pathologies. In an effort to produce clinically relevant results, we would recruit patients from a HF clinic and perform analysis to compare ROS data in ICM patients indicated for revascularization, ICM patients not indicated for revascularization, and NICM patients.

10. TABLES AND FIGURES

Table 1: Inclusion and Exclusion Criteria

Criteria	ICM Group	NICM group	All
Inclusion	• Diagnosis of ICM by CMR and/or angiography, clinical report used as standard of reference. See table 3 for list of diagnoses.	• Diagnosis of NICM by CMR, clinical report used as standard of reference. See table 3 for list of diagnoses.	• Age > 18 y • Informed consent
Exclusion	• General MRI contraindications including MR-incompatible pacemakers, intracranial aneurysm clips, metallic foreign bodies, and pregnancy. • Consumption of caffeine or vasoactive medications 12 hours before the CMR exam. • Unable to complete breathing maneuvers. • Hemodynamically unstable condition • Significant/uncontrolled arrhythmia		

Table 2: Subject Demographics

Clinical Characteristics	All (n=33)		ICM (n=20)		NICM (n=13)		P-Value
	Mean	**SD**	**Mean**	**SD**	**Mean**	**SD**	
Age (years)	61.0	14.1	62.6	14.1	58.5	14.3	0.421
*Male Sex (n)	27	81.8%	18	90.0%	9	69.2%	0.131
Height (cm)	172.5	8.5	173.6	7.4	170.8	10.1	0.366
Weight (kg)	81.8	19.0	83.9	21.3	78.6	15.0	0.443
Body Mass Index (kg/m^2)	27.4	5.9	27.8	6.8	26.8	4.3	0.633
Body Surface Area (m^2)	2.0	0.3	2.0	0.3	1.9	0.2	0.360
Heart Rate (beats/min)	69.4	13.3	67.9	13.4	71.7	13.4	0.434
Systolic Blood Pressure (mmHg)	139.6	18.7	138.7	22.4	141.1	11.6	0.722
Diastolic Blood Pressure (mmHg)	77.4	10.3	75.1	8.0	81.1	12.6	0.101
Co-Morbidities							
Hypertension	16		11		5		0.353
Diabetes Mellitus	7		5		2		>0.5
Dyslipidemia	11		8		3		0.314
Current Smoking	7		4		3		>0.5
Current Medications							
Ace Inhibitor	0		0		0		>0.5
Angiotensin Receptor Blocker	0		0		0		>0.5
Beta Blocker	0		0		0		>0.5
Diuretics	0		0		0		>0.5
Calcium Channel Blocker	0		0		0		>0.5
Statins	0		0		0		>0.5
Antiplatelet Medication	1		1		0		<0.5

*Values in Mean column represent number of males. Values in SD column represent the percentage of male sex.

Table 2: Functional Cardiovascular MRI Measurements

Parameter	All (n=33)		ICM (n=20)		NICM (n=13)		P-Value
	Mean	SD	Mean	SD	Mean	SD	
LV End-Diastolic Volume	129.5	46.5	138.6	53.2	115.6	30.6	0.169
LV End-Systolic Volume	54.6	43.1	63.9	52.1	40.5	17.1	0.130
LV Stroke Volume	74.6	21.4	74.1	22.8	75.3	20.0	0.877
LV Ejection Fraction	60.5	14.8	57.3	17.0	65.5	9.0	0.120
LV Mass	169.0	95.7	150.6	39.9	197.3	143.1	0.174
LV Cardiac Output	5.0	1.6	4.9	1.6	5.1	1.6	0.689
LV End-Diastolic Volume Index	65.4	22.3	69.2	26.8	59.4	11.3	0.224
LV End-Systolic Volume Index	27.8	22.1	32.4	27.0	20.7	7.2	0.137
LV Stroke Volume Index	37.0	10.2	36.8	11.1	37.3	9.1	0.890
LV Mass Index	83.0	49.6	70.4	23.2	102.4	71.0	0.070
LV Cardiac Output Index	2.5	0.7	2.4	0.8	2.6	0.6	0.421

Table 3: Cardiomyopathy Types by Clinical Report

Cardiomyopathy	Frequency
ICM (n=20)	
Inducible Perfusion Deficit	15
Ischemic Scar	5
NICM (n=13)	
Fibrosis	1
Hypertrophy	7
Infiltration	1
Inflammation	2
Noncompaction	1
Restrictive	1

Table 4: ROS Metrics in ICM vs NICM

A)

Metric	Overall Mean	95% CI	ICM Mean	95% CI2	NICM Mean	95% CI3	T-Test (p)
Global ΔSI%	4.59	0.70, 8.48	2.69	-3.33, 8.71	7.51	4.44, 10.58	0.241
Global SI Slope	0.08	0.02, 0.13	0.07	0.00, 0.14	0.09	-0.01, 0.19	>0.5
Global SD	4.48	4.05, 4.91	4.23	3.85, 4.62	4.84	3.94, 5.73	0.188
Global SD Slope	-0.02	-0.05, 0.01	0.00	-0.04, 0.04	-0.04	-0.09. 0.01	0.189
Minimum Segment ΔSI	-8.30	-11.28, -5.33	-10.10	-14.14, -5.79	-5.55	-8.80, -2.30	0.145
Segment ΔSI Range	20.58	17.8, 23.37	19.84	17.87, 27.57	21.09	17.34, 24.84	>0.5
Minimum Coronary Territory ΔSI	-4.68	-13.15, 3.79	-10.57	-23.17, 2.04	4.38	-3.06, 11.81	0.091
Coronary Territory ΔSI Range	20.81	18.2, 23.42	22.49	19.89, 25.09	18.49	13.45, 23.54	0.155

B)

Metric	AUC (ROC)	95% CI	AUC (p)	Chi-Square (p)	Simple Logistic Regression (p)
Global ΔSI%	0.696	0.511, 0.882	0.06	0.019	0.241
Global SI Slope	0.5423	0.337, 0.748	>0.5	>0.5	0.678
Global SD	0.583	0.366, 0.800	0.431		0.188
Global SD Slope	0.687	0.484, 0.889	0.074	>0.5	0.189
Minimum Segment ΔSI	0.6308	0.440, 0.822	0.21		0.145
Segment ΔSI Range	0.5425	0.333, 0.752	>0.5		0.679
Minimum Coronary Territory ΔSI	0.692	0.508, 0.877	0.065	0.027	0.091
Coronary Territory ΔSI Range	0.6154	0.396, 0.835	0.28		0.155

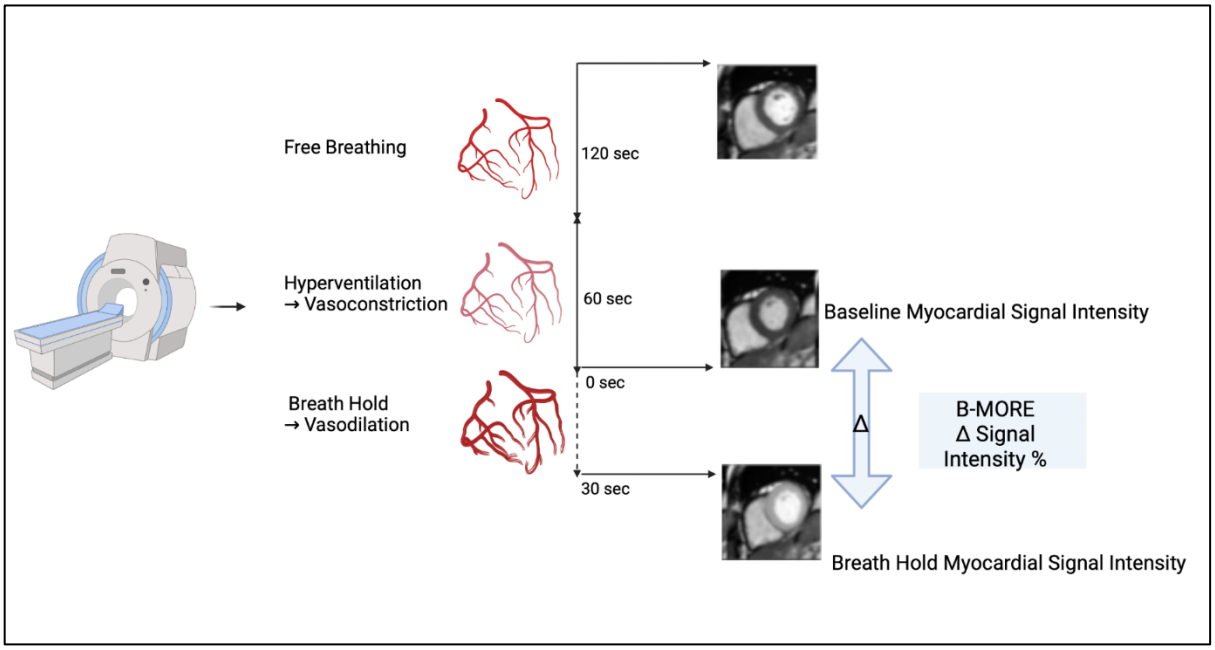

Figure 2: Myocardial oxygenation is assessed between the signal intensity of the first post-hyperventilation end-systolic image (at end of hypocapnia-induced vasoconstriction), and the signal intensity of the end-systolic image closest to 30 seconds into the BH, (during hypercapnia-induced vasodilation). Image courtesy of Kate Lindsay, created with BioRender.com

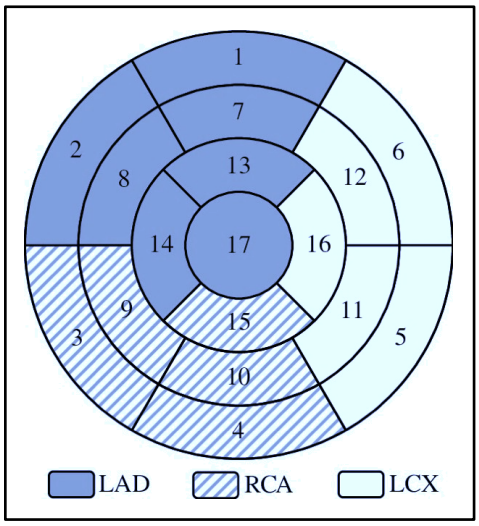

Figure 2: The 17-segment model for the segmentation of the LV as presented by the AHA. The patterns indicate the mapping of the segments to coronary territories (106).

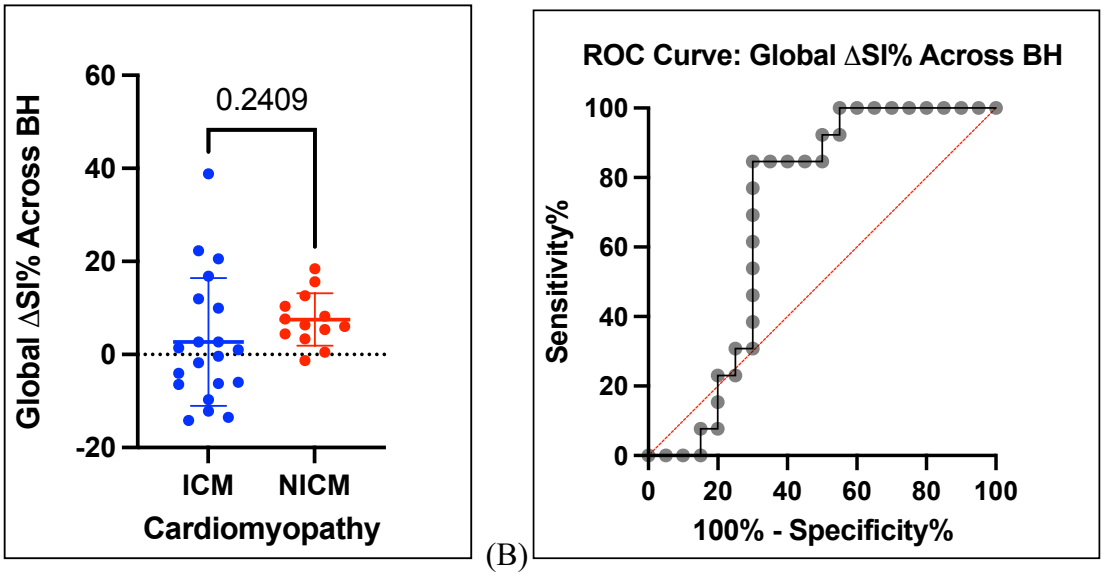

Figure 3: (A) The overall mean ΔSI% over the BH (B-MORE) was 4.59 (CI 0.7, 8.48). Though not statistically significant in a t-test (p=0.241), mean B-MORE was decreased in ICM at 2.69 (CI -3.33, 8.71) compared to 7.51 in NICM (CI 4.44, 10.58). When treated as a binomial for either positive change or negative change in global SI (seen as above or below the dotted line, respectively in, ICM showed negative changes in 10 (50%) subjects, while NICM showed negative changes in 1 (8%) subject. This difference was significant in a chi-square statistic (p=0.019). (B) In ROC analysis, AUC was 0.696 (CI 0.511, 0.882), p=0.060.

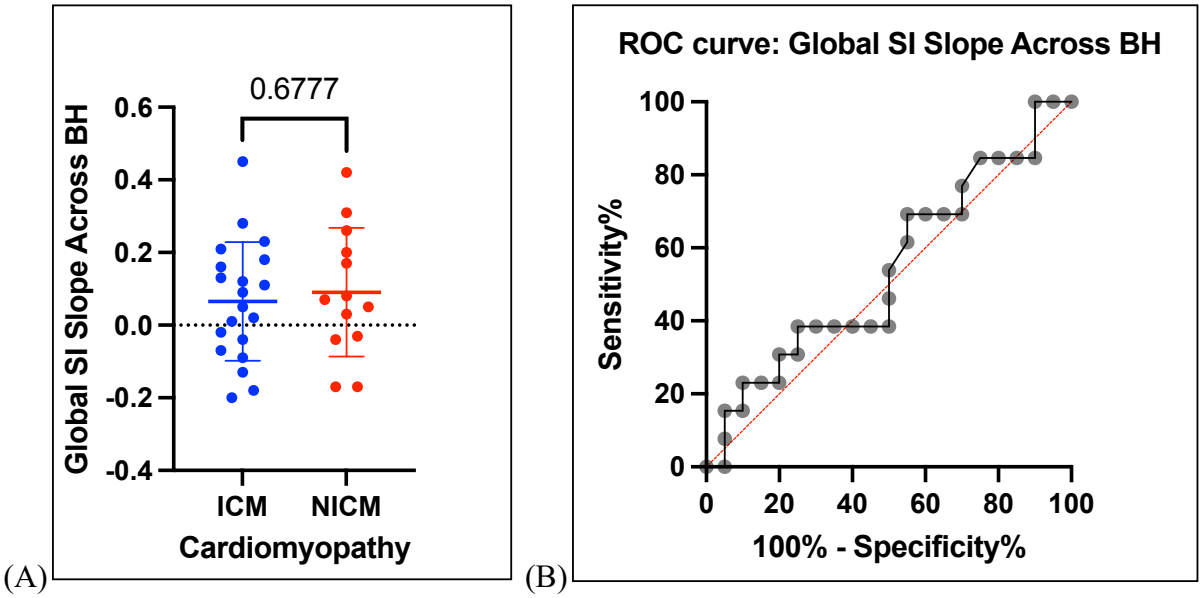

Figure 4: (A) The overall mean slope of the average global SI across the BH was 0.08 (CI 0.02, 0.13). This value was not significantly different (p>0.5) between ICM (0.07; CI 0.00, 0.14) and NICM (0.09; CI -0.01, 0.19). Assessment of this metric as a positive or negative binomial yielded no significant difference between ICM and NICM in a chi-square statistic (p>0.5). (B) In ROC analysis, AUC was 0.5423 (CI 0.337, 0.748), p>0.5.

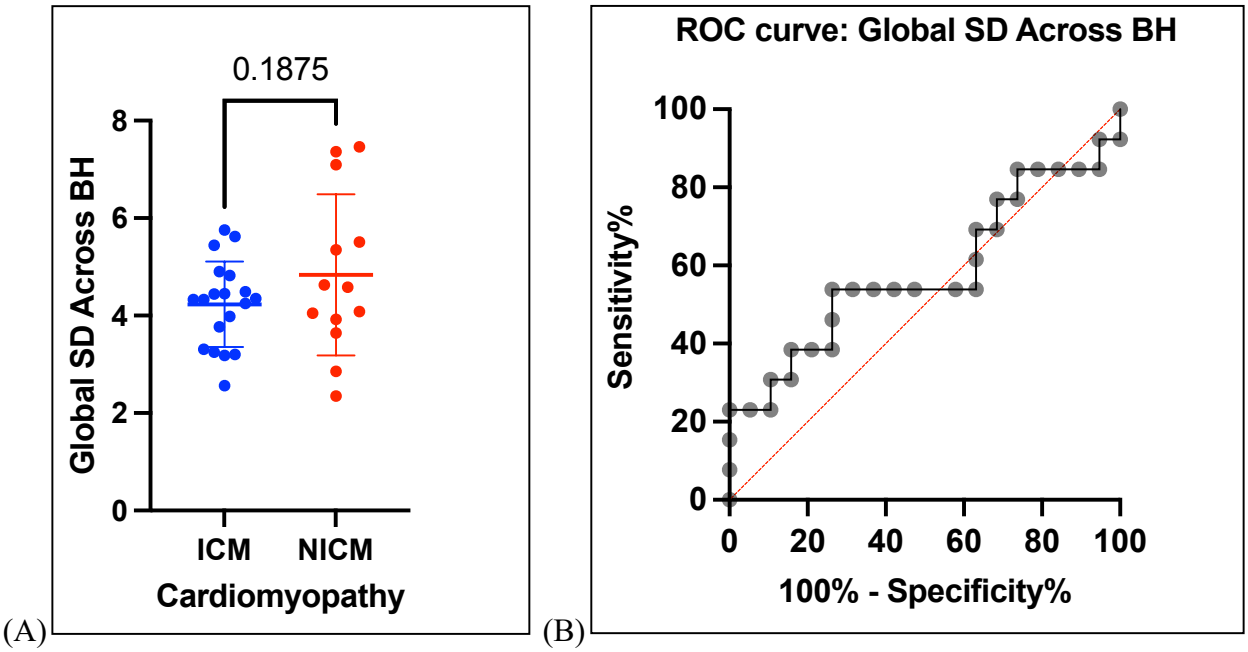

Figure 5: (A) The overall mean of global SD across the BH was 4.48 (CI 4.05, 4.91). The value was not significantly different between (p=0.188) between ICM (4.23; CI 3.85, 4.62) and NICM (4.84; CI 3.94, 5.73). (B) In ROC analysis, AUC was 0.5830 (CI 0.3660, 0.8000), p=0.431. One statistically significant outlier was excluded from this analysis (ICM; 9.43).

(A)

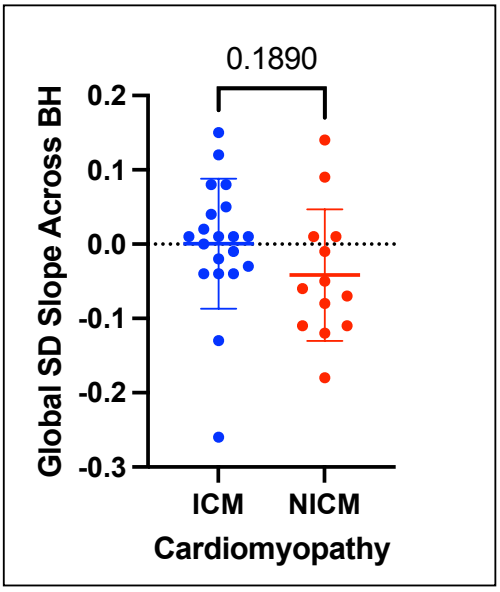

(B)

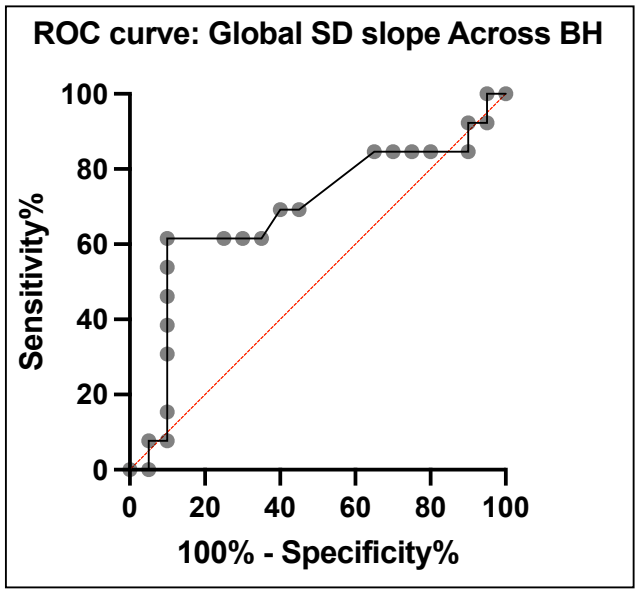

Figure 6: (A) The overall mean slope of global SD across the BH was -0.02 (CI -0.05, 0.01). This value was not significantly different (p=0.189) between ICM (0.00; CI -0.04, 0.04) and NICM (-0.04; CI -0.09, 0.01). Assessment of this metric as a binomial yielded no significant difference in a chi-square statistic (p>0.5). (B) In ROC analysis, AUC was 0.687 (CI 0.484, 0.889), p=0.074.

(A)

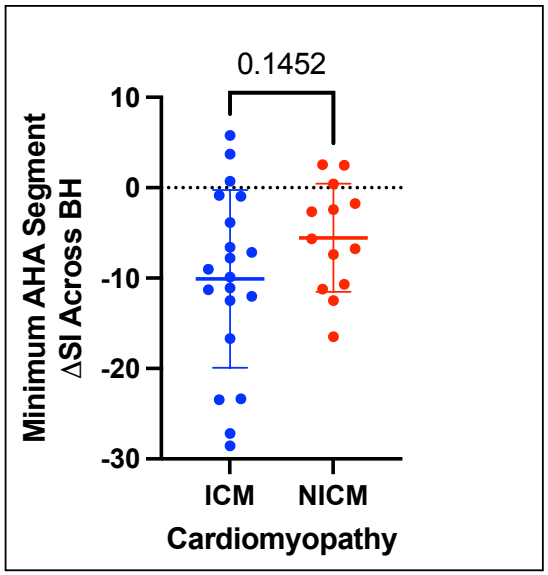

(B)

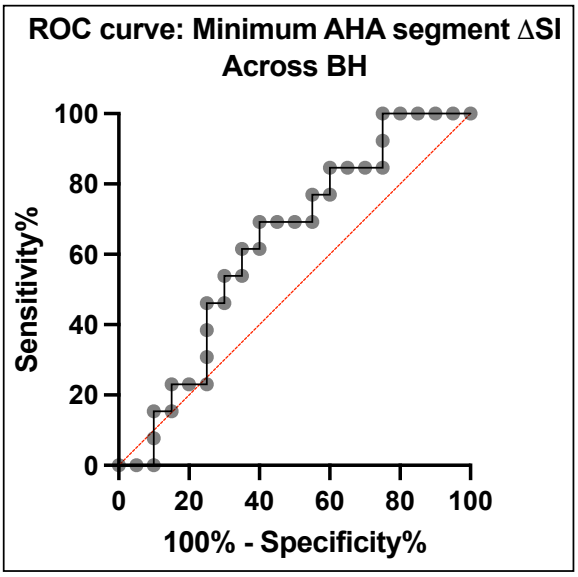

Figure 7: (A) *The overall mean of minimum segment change was -8.30 (CI -11.28, -5.33). The mean values in ICM were decreased compared to NICM were -10.10 (CI -14.41, -5.79) and -5.55 (CI -8.8, -2.3), respectively. This difference was notable but not statistically significant with p=0.145. (B) In ROC analysis, AUC was 0.6308 (CI 0.4395, 0.8220), p=0.210.*

(A)

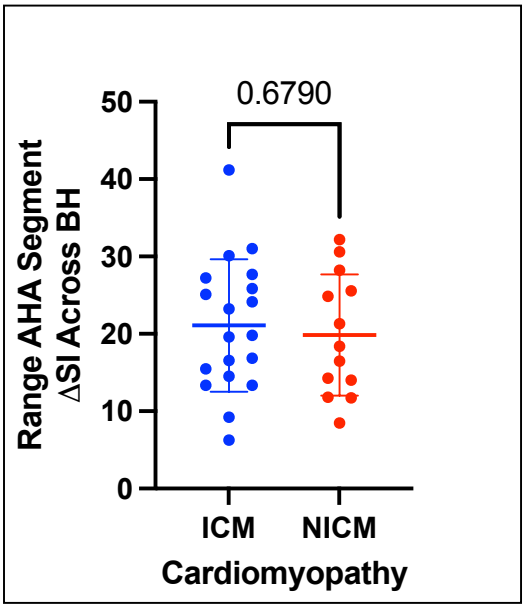

(B)

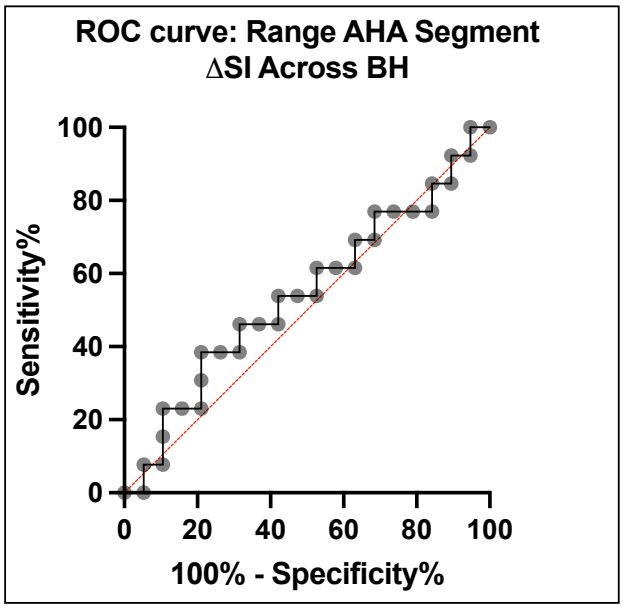

Figure 8: (A) *The overall mean of the range of segment change was 20.58 (CI 17.8, 23.37). The mean values in ICM and NICM were 19.84 (CI 17.87, 27.57) and 21.09 (CI 17.34, 24.84), respectively. This difference was not statistically significant (p>0.5).(B) In ROC analysis, AUC was 0.5425 (CI 0.3329, 0.7521), p>0.5. One statistically significant outlier was excluded from this analysis (ICM; 53.71).*

(A)

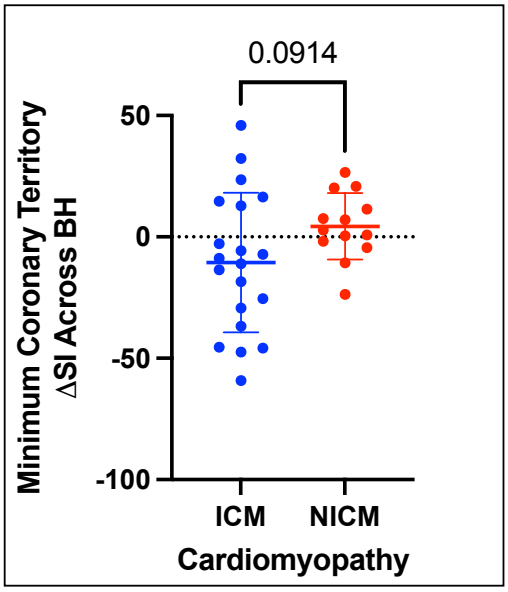

(B)

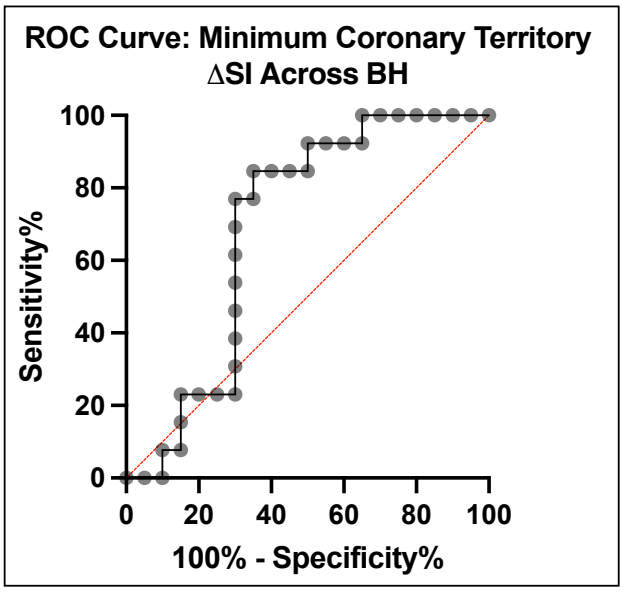

Figure 9: (A) *The overall mean of minimum coronary territory change was -4.68 (CI -13.15, 3.79). The mean values were decreased in in ICM (-10.57; CI -23.17, 2.04) compared to NICM (4.38; CI -3.06, 11.81). This difference was notable but not statistically significant with p=0.091. When treated as a binomial for either positive change or negative change, ICM showed negative changes in 14 (70%) subjects, while NICM showed negative changes in 4 (31%) subjects. This difference was significant in a chi-square statistic (p= 0.027). (B) In ROC analysis, AUC was 0.692 (CI 0.508, 0.877), p=0.065.*

(A)

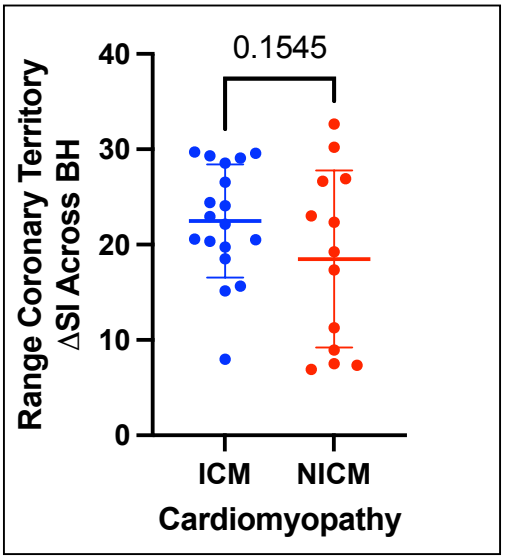

(B)

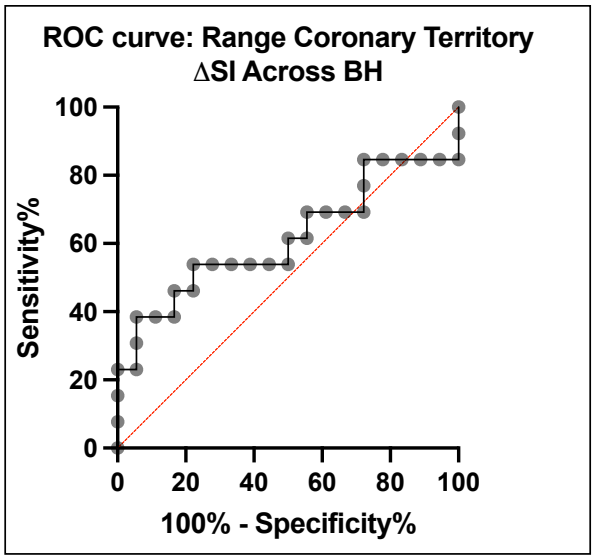

Figure 10: (A) The overall mean of the range of coronary territory change was 20.81 (CI 18.2, 23.42). The mean values were increased in ICM (22.49; CI 19.89, 25.09) compared to NICM (18.49; CI 13.45, 23.54), respectively. This difference was notable but not statistically significant p=0.155. (B) In ROC analysis, AUC was 0.6154 (CI 0.3959, 0.8349), p=0.280. Two statistically significant outliers were excluded from this analysis (ICM; 85.6, 66.47).

11. DECLARATIONS

Conflicts of Interest

MGF is a shareholder, and consultant of Circle Cardiovascular Imaging Inc. and Area 19 Medical Inc. He is also listed as a holder of: United States Patent No. 14/419,877: Inducing and measuring myocardial oxygenation changes as a marker for heart disease; United States Patent No. 15/483,712: Measuring oxygenation changes in tissue as a marker for vascular function; United States Patent No 10,653,394: Measuring oxygenation changes in tissue as a marker for vascular function - continuation; Canadian Patent CA2020/051776: Method and apparatus for determining biomarkers of vascular function utilizing bold CMR images. EH is listed as a holder of Canadian Patent CA2020/051776: Method and apparatus for determining biomarkers of vascular function utilizing bold CMR images. The other authors report no conflicts.

12. REFERENCES

1. Braunwald E. Heart failure. JACC Heart Fail. 2013 Feb;1(1):1–20.

2. Shah KS, Xu H, Matsouaka RA, Bhatt DL, Heidenreich PA, Hernandez AF, et al. Heart Failure With Preserved, Borderline, and Reduced Ejection Fraction: 5-Year Outcomes. J Am Coll Cardiol. 2017 Nov 14;70(20):2476–86.

3. Groenewegen A, Rutten FH, Mosterd A, Hoes AW. Epidemiology of heart failure. Eur J Heart Fail. 2020 Aug;22(8):1342–56.

4. Ambrosy AP, Fonarow GC, Butler J, Chioncel O, Greene SJ, Vaduganathan M, et al. The global health and economic burden of hospitalizations for heart failure: lessons learned from hospitalized heart failure registries. J Am Coll Cardiol. 2014 Apr 1;63(12):1123–33.

5. Ferreira JP, Kraus S, Mitchell S, Perel P, Piñeiro D, Chioncel O, et al. World Heart Federation Roadmap for Heart Failure. Glob Heart. 2019 Sep;14(3):197–214.

6. Savarese G, Stolfo D, Sinagra G, Lund LH. Heart failure with mid-range or mildly reduced ejection fraction. Nat Rev Cardiol [Internet]. 2021 Sep 6; Available from: http://dx.doi.org/10.1038/s41569-021-00605-5

7. Patel J. Heart failure population health considerations. Am J Manag Care. 2021 Jun;27(9 Suppl):S191–5.

8. Jackson SL, Tong X, King RJ, Loustalot F, Hong Y, Ritchey MD. National Burden of Heart Failure Events in the United States, 2006 to 2014. Circ Heart Fail. 2018 Dec;11(12):e004873.

9. Ciarambino T, Menna G, Sansone G, Giordano M. Cardiomyopathies: An Overview. Int J Mol Sci [Internet]. 2021 Jul 19;22(14). Available from: http://dx.doi.org/10.3390/ijms22147722

10. Bluemke DA. MRI of nonischemic cardiomyopathy. AJR Am J Roentgenol. 2010 Oct;195(4):935–40.

11. Bhandari B, Quintanilla Rodriguez BS, Masood W. Ischemic Cardiomyopathy. In: StatPearls. Treasure Island (FL): StatPearls Publishing; 2021.

12. Wu AH. Management of patients with non-ischaemic cardiomyopathy. Heart. 2007 Mar;93(3):403–8.

13. Ponikowski P, Voors AA, Anker SD, Bueno H, Cleland JGF, Coats AJS, et al. 2016 ESC Guidelines for the diagnosis and treatment of acute and chronic heart failure: The Task Force for the diagnosis and treatment of acute and chronic heart failure of the European Society of Cardiology (ESC)Developed with the special contribution of the Heart Failure Association (HFA) of the ESC. Eur Heart J. 2016 Jul 14;37(27):2129–200.

14. Mahmaljy H, Yelamanchili VS, Singhal M. Dilated Cardiomyopathy. In: StatPearls. Treasure Island (FL): StatPearls Publishing; 2021.

15. Zuchi C, Tritto I, Carluccio E, Mattei C, Cattadori G, Ambrosio G. Role of endothelial dysfunction in heart failure. Heart Fail Rev. 2020 Jan;25(1):21–30.

16. Dryer K, Gajjar M, Narang N, Lee M, Paul J, Shah AP, et al. Coronary microvascular dysfunction in patients with heart failure with preserved ejection fraction. Am J Physiol Heart Circ Physiol. 2018 May 1;314(5):H1033–42.

17. Franssen C, Chen S, Unger A, Korkmaz HI, De Keulenaer GW, Tschöpe C, et al. Myocardial Microvascular Inflammatory Endothelial Activation in Heart Failure With Preserved Ejection Fraction. JACC Heart Fail. 2016 Apr;4(4):312–24.

18. Shah SJ, Lam CSP, Svedlund S, Saraste A, Hage C, Tan R-S, et al. Prevalence and correlates of coronary microvascular dysfunction in heart failure with preserved ejection fraction: PROMIS-HFpEF. Eur Heart J. 2018 Oct 1;39(37):3439–50.

19. Taqueti VR, Di Carli MF. Coronary Microvascular Disease Pathogenic Mechanisms and Therapeutic Options: JACC State-of-the-Art Review. J Am Coll Cardiol. 2018 Nov 27;72(21):2625–41.

20. Katz SD, Hryniewicz K, Hriljac I, Balidemaj K, Dimayuga C, Hudaihed A, et al. Vascular endothelial dysfunction and mortality risk in patients with chronic heart failure. Circulation. 2005 Jan 25;111(3):310–4.

21. Godo S, Suda A, Takahashi J, Yasuda S, Shimokawa H. Coronary Microvascular Dysfunction. Arterioscler Thromb Vasc Biol. 2021 May 5;41(5):1625–37.

22. Sun H-J, Wu Z-Y, Nie X-W, Bian J-S. Role of Endothelial Dysfunction in Cardiovascular Diseases: The Link Between Inflammation and Hydrogen Sulfide. Front Pharmacol. 2019;10:1568.

23. Giannotti G, Landmesser U. Endothelial dysfunction as an early sign of atherosclerosis. Herz. 2007 Oct;32(7):568–72.

24. Bui AL, Horwich TB, Fonarow GC. Epidemiology and risk profile of heart failure. Nat Rev Cardiol. 2011 Jan;8(1):30–41.

25. Malik A, Brito D, Chhabra L. Congestive Heart Failure. In: StatPearls. Treasure Island (FL): StatPearls Publishing; 2021.

26. Udelson JE. Cardiac Magnetic Resonance Imaging for Long-Term Prognosis in Heart Failure. Circ Cardiovasc Imaging. 2018 Sep;11(9):e008264.

27. Bozkurt B, Coats AJS, Tsutsui H, Abdelhamid CM, Adamopoulos S, Albert N, et al. Universal definition and classification of heart failure: a report of the Heart Failure Society of America, Heart Failure Association of the European Society of Cardiology, Japanese

Heart Failure Society and Writing Committee of the Universal Definition of Heart Failure: Endorsed by the Canadian Heart Failure Society, Heart Failure Association of India, Cardiac Society of Australia and New Zealand, and Chinese Heart Failure Association. Eur J Heart Fail. 2021 Mar;23(3):352–80.

28. Singh P, Bhatt B, Pawar SU, Kamra A, Shetye S, Ghorpade M. Role of Myocardial Perfusion Study in Differentiating Ischemic versus Nonischemic Cardiomyopathy Using Quantitative Parameters. Indian J Nucl Med. 2018 Jan;33(1):32–8.

29. Moreno R, 'ovidio AD, Zamorano J, Almería C, Macaya C. Distinguishing between ischemic and non-ischemic dilated cardiomyopathy based on non-invasive ultrasonic evaluation of peripheral arteries. Eur J Intern Med. 2005 Feb;16(1):41–6.

30. Sawada SG, Ryan T, Segar D, Atherton L, Fineberg N, Davis C, et al. Distinguishing ischemic cardiomyopathy from nonischemic dilated cardiomyopathy with coronary echocardiography. J Am Coll Cardiol. 1992 May;19(6):1223–8.

31. Corbalan R, Bassand J-P, Illingworth L, Ambrosio G, Camm AJ, Fitzmaurice DA, et al. Analysis of Outcomes in Ischemic vs Nonischemic Cardiomyopathy in Patients With Atrial Fibrillation: A Report From the GARFIELD-AF Registry. JAMA Cardiol. 2019 Jun 1;4(6):526–48.

32. Perera D, Clayton T, Petrie MC, Greenwood JP, O'Kane PD, Evans R, et al. Percutaneous Revascularization for Ischemic Ventricular Dysfunction: Rationale and Design of the REVIVED-BCIS2 Trial: Percutaneous Coronary Intervention for Ischemic Cardiomyopathy. JACC Heart Fail. 2018 Jun;6(6):517–26.

33. Maggioni AP, Dahlström U, Filippatos G, Chioncel O, Crespo Leiro M, Drozdz J, et al. EURObservational Research Programme: regional differences and 1-year follow-up results of the Heart Failure Pilot Survey (ESC-HF Pilot). Eur J Heart Fail. 2013 Jul;15(7):808–17.

34. Bart BA, Shaw LK, McCants CB Jr, Fortin DF, Lee KL, Califf RM, et al. Clinical determinants of mortality in patients with angiographically diagnosed ischemic or nonischemic cardiomyopathy. J Am Coll Cardiol. 1997 Oct;30(4):1002–8.

35. Assomull RG, Shakespeare C, Kalra PR, Lloyd G, Gulati A, Strange J, et al. Role of cardiovascular magnetic resonance as a gatekeeper to invasive coronary angiography in patients presenting with heart failure of unknown etiology. Circulation. 2011 Sep 20;124(12):1351–60.

36. Cowie MR, Anker SD, Cleland JGF, Felker GM, Filippatos G, Jaarsma T, et al. Improving care for patients with acute heart failure: before, during and after hospitalization. ESC Heart Fail. 2014 Dec;1(2):110–45.

37. Čerlinskaitė K, Javanainen T, Cinotti R, Mebazaa A, Global Research on Acute Conditions Team (GREAT) Network. Acute Heart Failure Management. Korean Circ J. 2018 Jun;48(6):463–80.

38. Sado DM, Hasleton JM, Herrey AS, Moon JC. CMR in Heart Failure. Cardiol Res Pract. 2011 Aug 16;2011:739157.

39. Tavakol M, Ashraf S, Brener SJ. Risks and complications of coronary angiography: a comprehensive review. Glob J Health Sci. 2012 Jan 1;4(1):65–93.

40. Farrehi PM, Bernstein SJ, Rasak M, Dabbous SA, Stomel RJ, Eagle KA, et al. Frequency of negative coronary arteriographic findings in patients with chest pain is related to community practice patterns. Am J Manag Care. 2002 Jul;8(7):643–8.

41. Gulati M, Cooper-DeHoff RM, McClure C, Johnson BD, Shaw LJ, Handberg EM, et al. Adverse cardiovascular outcomes in women with nonobstructive coronary artery disease: a report from the Women's Ischemia Syndrome Evaluation Study and the St James Women Take Heart Project. Arch Intern Med. 2009 May 11;169(9):843–50.

42. Herscovici R, Sedlak T, Wei J, Pepine CJ, Handberg E, Bairey Merz CN. Ischemia and No Obstructive Coronary Artery Disease (INOCA): What Is the Risk? J Am Heart Assoc. 2018 Sep 4;7(17):e008868.

43. Vancheri F, Longo G, Vancheri S, Henein M. Coronary Microvascular Dysfunction. J Clin Med Res [Internet]. 2020 Sep 6;9(9). Available from: http://dx.doi.org/10.3390/jcm9092880

44. Vaquero JJ, Kinahan P. Positron Emission Tomography: Current Challenges and Opportunities for Technological Advances in Clinical and Preclinical Imaging Systems. Annu Rev Biomed Eng. 2015;17:385–414.

45. Nissen Steven E. Limitations of Computed Tomography Coronary Angiography∗. J Am Coll Cardiol. 2008 Dec 16;52(25):2145–7.

46. Hsu L-Y, Jacobs M, Benovoy M, Ta AD, Conn HM, Winkler S, et al. Diagnostic Performance of Fully Automated Pixel-Wise Quantitative Myocardial Perfusion Imaging by Cardiovascular Magnetic Resonance. JACC Cardiovasc Imaging. 2018 May;11(5):697–707.

47. Grover VPB, Tognarelli JM, Crossey MME, Cox IJ, Taylor-Robinson SD, McPhail MJW. Magnetic Resonance Imaging: Principles and Techniques: Lessons for Clinicians. J Clin Exp Hepatol. 2015 Sep;5(3):246–55.

48. Seeger LL. Physical principles of magnetic resonance imaging. Clin Orthop Relat Res. 1989 Jul;(244):7–16.

49. McGowan JC. Basic principles of magnetic resonance imaging. Neuroimaging Clin N Am. 2008 Nov;18(4):623–36, x.

50. Barison A, Aimo A, Todiere G, Grigoratos C, Aquaro GD, Emdin M. Cardiovascular magnetic resonance for the diagnosis and management of heart failure with preserved ejection fraction. Heart Fail Rev [Internet]. 2020 Jun 22; Available from: http://dx.doi.org/10.1007/s10741-020-09998-w

51. Mitropoulou P, Georgiopoulos G, Figliozzi S, Klettas D, Nicoli F, Masci PG. Multi-Modality Imaging in Dilated Cardiomyopathy: With a Focus on the Role of Cardiac Magnetic Resonance. Front Cardiovasc Med. 2020 Jul 2;7:97.

52. Karamitsos TD, Arvanitaki A, Karvounis H, Neubauer S, Ferreira VM. Myocardial Tissue Characterization and Fibrosis by Imaging. JACC Cardiovasc Imaging. 2020 May;13(5):1221–34.

53. Le Ven F, Bibeau K, De Larochellière É, Tizón-Marcos H, Deneault-Bissonnette S, Pibarot P, et al. Cardiac morphology and function reference values derived from a large subset of healthy young Caucasian adults by magnetic resonance imaging. Eur Heart J Cardiovasc Imaging. 2016 Sep;17(9):981–90.

54. Simpson R, Bromage D, Dancy L, McDiarmid A, Monaghan M, McDonagh T, et al. 6 Comparing echocardiography and cardiac magnetic resonance measures of ejection fraction: implications for HFMRF research. Heart. 2018 May 1;104(Suppl 5):A3–A3.

55. Paterson DI, Wells G, Erthal F, Mielniczuk L, O'Meara E, White J, et al. OUTSMART HF: A Randomized Controlled Trial of Routine Versus Selective Cardiac Magnetic Resonance for Patients With Nonischemic Heart Failure (IMAGE-HF 1B). Circulation. 2020 Mar 10;141(10):818–27.

56. Kanagala P, Cheng ASH, Singh A, McAdam J, Marsh A-M, Arnold JR, et al. Diagnostic and prognostic utility of cardiovascular magnetic resonance imaging in heart failure with preserved ejection fraction - implications for clinical trials. J Cardiovasc Magn Reson. 2018 Jan 11;20(1):4.

57. Bhuiyan T, Maurer MS. Heart Failure with Preserved Ejection Fraction: Persistent Diagnosis, Therapeutic Enigma. Curr Cardiovasc Risk Rep. 2011 Oct;5(5):440–9.

58. Reiter T, Ritter O, Prince MR, Nordbeck P, Wanner C, Nagel E, et al. Minimizing risk of nephrogenic systemic fibrosis in cardiovascular magnetic resonance. J Cardiovasc Magn Reson. 2012 May 20;14:31.

59. Pilz G, Patel PA, Fell U, Ladapo JA, Rizzo JA, Fang H, et al. Adenosine-stress cardiac magnetic resonance imaging in suspected coronary artery disease: a net cost analysis and reimbursement implications. Int J Cardiovasc Imaging. 2011 Jan;27(1):113–21.

60. Kwong RY, Ge Y, Steel K, Bingham S, Abdullah S, Fujikura K, et al. Cardiac Magnetic Resonance Stress Perfusion Imaging for Evaluation of Patients With Chest Pain. J Am Coll Cardiol. 2019 Oct 8;74(14):1741–55.

61. Nagel E, Greenwood JP, McCann GP, Bettencourt N, Shah AM, Hussain ST, et al. Magnetic Resonance Perfusion or Fractional Flow Reserve in Coronary Disease. N Engl J Med. 2019 Jun 20;380(25):2418–28.

62. Manka R, Paetsch I, Schnackenburg B, Gebker R, Fleck E, Jahnke C. BOLD cardiovascular magnetic resonance at 3.0 tesla in myocardial ischemia. J Cardiovasc Magn Reson. 2010 Sep 22;12:54.

63. Buxton RB. The physics of functional magnetic resonance imaging (fMRI). Rep Prog Phys. 2013 Sep;76(9):096601.

64. Ogawa S, Lee TM, Kay AR, Tank DW. Brain magnetic resonance imaging with contrast dependent on blood oxygenation. Proc Natl Acad Sci U S A. 1990 Dec;87(24):9868–72.

65. Sree Raman K, Nucifora G, Selvanayagam JB. Novel cardiovascular magnetic resonance oxygenation approaches in understanding pathophysiology of cardiac diseases. Clin Exp Pharmacol Physiol. 2018 May;45(5):475–80.

66. Ochs MM, Kajzar I, Salatzki J, Ochs AT, Riffel J, Osman N, et al. Hyperventilation/Breath-Hold Maneuver to Detect Myocardial Ischemia by Strain-Encoded CMR: Diagnostic Accuracy of a Needle-Free Stress Protocol. JACC Cardiovasc Imaging [Internet]. 2021 Apr 7; Available from: http://dx.doi.org/10.1016/j.jcmg.2021.02.022

67. Duncker DJ, Bache RJ. Regulation of coronary blood flow during exercise. Physiol Rev. 2008 Jul;88(3):1009–86.

68. Ogawa S, Tank DW, Menon R, Ellermann JM, Kim SG, Merkle H, et al. Intrinsic signal changes accompanying sensory stimulation: functional brain mapping with magnetic resonance imaging. Proc Natl Acad Sci U S A. 1992 Jul 1;89(13):5951–5.

69. Barac A, Campia U, Panza JA. Methods for evaluating endothelial function in humans. Hypertension. 2007 Apr;49(4):748–60.

70. Fischer K, Guensch DP, Friedrich MG. Response of myocardial oxygenation to breathing manoeuvres and adenosine infusion. Eur Heart J Cardiovasc Imaging. 2015 Apr;16(4):395–401.

71. Singh S, McKintosh R. Adenosine. In: StatPearls. Treasure Island (FL): StatPearls Publishing; 2021.

72. Durand MJ, Gutterman DD. Diversity in mechanisms of endothelium-dependent vasodilation in health and disease. Microcirculation. 2013 Apr;20(3):239–47.

73. Hadi HAR, Carr CS, Al Suwaidi J. Endothelial dysfunction: cardiovascular risk factors, therapy, and outcome. Vasc Health Risk Manag. 2005;1(3):183–98.

74. Shantsila E, Wrigley BJ, Blann AD, Gill PS, Lip GYH. A contemporary view on endothelial function in heart failure. Eur J Heart Fail. 2012 Aug;14(8):873–81.

75. Giannitsi S, Bougiakli M, Bechlioulis A, Naka K. Endothelial dysfunction and heart failure: A review of the existing bibliography with emphasis on flow mediated dilation. JRSM Cardiovasc Dis. 2019 Jan;8:2048004019843047.

76. Fischer D, Rossa S, Landmesser U, Spiekermann S, Engberding N, Hornig B, et al. Endothelial dysfunction in patients with chronic heart failure is independently associated with increased incidence of hospitalization, cardiac transplantation, or death. Eur Heart J. 2005 Jan;26(1):65–9.

77. Hasdai D, Cannan CR, Mathew V, Holmes DR Jr, Lerman A. Evaluation of patients with minimally obstructive coronary artery disease and angina. Int J Cardiol. 1996 Mar;53(3):203–8.

78. Zeiher AM, Drexler H, Wollschlaeger H, Saurbier B, Just H. Coronary vasomotion in response to sympathetic stimulation in humans: importance of the functional integrity of the endothelium. J Am Coll Cardiol. 1989 Nov 1;14(5):1181–90.

79. Moreton FC, Dani KA, Goutcher C, O'Hare K, Muir KW. Respiratory challenge MRI: Practical aspects. Neuroimage Clin. 2016 May 6;11:667–77.

80. Kety SS, Schmidt CF. THE EFFECTS OF ALTERED ARTERIAL TENSIONS OF CARBON DIOXIDE AND OXYGEN ON CEREBRAL BLOOD FLOW AND CEREBRAL OXYGEN CONSUMPTION OF NORMAL YOUNG MEN. J Clin Invest. 1948 Jul;27(4):484–92.

81. Winklhofer S, Pazahr S, Manka R, Alkadhi H, Boss A, Stolzmann P. Quantitative blood oxygenation level-dependent (BOLD) response of the left ventricular myocardium to hyperoxic respiratory challenge at 1.5 and 3.0 T. NMR Biomed. 2014 Jul;27(7):795–801.

82. Stalder AF, Schmidt M, Greiser A, Speier P, Guehring J, Friedrich MG, et al. Robust cardiac BOLD MRI using an fMRI-like approach with repeated stress paradigms. Magn Reson Med. 2015 Feb;73(2):577–85.

83. Patel S, Miao JH, Yetiskul E, Anokhin A, Majmundar SH. Physiology, Carbon Dioxide Retention. In: StatPearls. Treasure Island (FL): StatPearls Publishing; 2021.

84. Guensch DP, Fischer K, Flewitt JA, Yu J, Lukic R, Friedrich JA, et al. Breathing manoeuvre-dependent changes in myocardial oxygenation in healthy humans. Eur Heart J Cardiovasc Imaging. 2014 Apr;15(4):409–14.

85. Teixeira T, Nadeshalingam G, Fischer K, Marcotte F, Friedrich MG. Breathing maneuvers as a coronary vasodilator for myocardial perfusion imaging. J Magn Reson Imaging. 2016 Oct;44(4):947–55.

86. Guensch DP, Fischer K, Flewitt JA, Friedrich MG. Myocardial oxygenation is maintained during hypoxia when combined with apnea - a cardiovascular MR study. Physiol Rep. 2013 Oct;1(5):e00098.

87. Fischer K, Guensch DP, Shie N, Lebel J, Friedrich MG. Breathing Maneuvers as a Vasoactive Stimulus for Detecting Inducible Myocardial Ischemia - An Experimental Cardiovascular Magnetic Resonance Study. PLoS One. 2016 Oct 14;11(10):e0164524.

88. Fischer K, Yamaji K, Luescher S, Ueki Y, Jung B, von Tengg-Kobligk H, et al. Feasibility of cardiovascular magnetic resonance to detect oxygenation deficits in patients with multi-vessel coronary artery disease triggered by breathing maneuvers. J Cardiovasc Magn Reson. 2018 May 7;20(1):31.

89. Elharram M, Hillier E, Hawkins S, Mikami Y, Heydari B, Merchant N, et al. Regional Heterogeneity in the Coronary Vascular Response in Women With Chest Pain and Nonobstructive Coronary Artery Disease. Circulation. 2021 Feb 16;143(7):764–6.

90. Walcher T, Manzke R, Hombach V, Rottbauer W, Wöhrle J, Bernhardt P. Myocardial perfusion reserve assessed by T2-prepared steady-state free precession blood oxygen level-dependent magnetic resonance imaging in comparison to fractional flow reserve. Circ Cardiovasc Imaging. 2012 Sep 1;5(5):580–6.

91. Karamitsos TD, Leccisotti L, Arnold JR, Recio-Mayoral A, Bhamra-Ariza P, Howells RK, et al. Relationship between regional myocardial oxygenation and perfusion in patients with coronary artery disease: insights from cardiovascular magnetic resonance and positron emission tomography. Circ Cardiovasc Imaging. 2010 Jan;3(1):32–40.

92. Arnold JR, Karamitsos TD, Bhamra-Ariza P, Francis JM, Searle N, Robson MD, et al. Myocardial oxygenation in coronary artery disease: insights from blood oxygen level-dependent magnetic resonance imaging at 3 tesla. J Am Coll Cardiol. 2012 May 29;59(22):1954–64.

93. Luu JM, Friedrich MG, Harker J, Dwyer N, Guensch D, Mikami Y, et al. Relationship of vasodilator-induced changes in myocardial oxygenation with the severity of coronary artery stenosis: a study using oxygenation-sensitive cardiovascular magnetic resonance. Eur Heart J Cardiovasc Imaging. 2014 Dec;15(12):1358–67.

94. Maron DJ, Hochman JS, Reynolds HR, Bangalore S, O'Brien SM, Boden WE, et al. Initial Invasive or Conservative Strategy for Stable Coronary Disease. N Engl J Med. 2020 Apr 9;382(15):1395–407.

95. Kothawade K, Bairey Merz CN. Microvascular coronary dysfunction in women: pathophysiology, diagnosis, and management. Curr Probl Cardiol. 2011 Aug;36(8):291–318.

96. Lanza GA. Cardiac syndrome X: a critical overview and future perspectives. Heart. 2007 Feb;93(2):159–66.

97. Iannino N, Fischer K, Friedrich M, Hafyane T, Mongeon F-P, White M. Myocardial Vascular Function Assessed by Dynamic Oxygenation-sensitive Cardiac Magnetic Resonance Imaging Long-term Following Cardiac Transplantation. Transplantation. 2021 Jun 1;105(6):1347–55.

98. Mahmod M, Francis JM, Pal N, Lewis A, Dass S, De Silva R, et al. Myocardial perfusion and oxygenation are impaired during stress in severe aortic stenosis and correlate with

impaired energetics and subclinical left ventricular dysfunction. J Cardiovasc Magn Reson. 2014 Apr 29;16:29.

99. Roubille F, Fischer K, Guensch DP, Tardif J-C, Friedrich MG. Impact of hyperventilation and apnea on myocardial oxygenation in patients with obstructive sleep apnea - An oxygenation-sensitive CMR study. J Cardiol. 2017 Feb;69(2):489–94.

100. Raman B, Chan K, Ariga R, Mahmod M, Hundertmark M, Sivalokanathan S, et al. Abstract 10875: Impaired Stress Myocardial Oxygenation and Not Perfusion Reserve is Associated With Arrhythmic Risk in Hypertrophic Cardiomyopathy: Insights From a Novel Oxygen Sensitive Cardiac Magnetic Resonance Approach. Circulation. 2019 Nov 19;140(Suppl_1):A10875–A10875.

101. Karamitsos TD, Dass S, Suttie J, Sever E, Birks J, Holloway CJ, et al. Blunted myocardial oxygenation response during vasodilator stress in patients with hypertrophic cardiomyopathy. J Am Coll Cardiol. 2013 Mar 19;61(11):1169–76.

102. McMurray JJV, Adamopoulos S, Anker SD, Auricchio A, Böhm M, Dickstein K, et al. ESC Guidelines for the diagnosis and treatment of acute and chronic heart failure 2012: The Task Force for the Diagnosis and Treatment of Acute and Chronic Heart Failure 2012 of the European Society of Cardiology. Developed in collaboration with the Heart Failure Association (HFA) of the ESC. Eur Heart J. 2012 Jul;33(14):1787–847.

103. Savarese G, Lund LH. Global Public Health Burden of Heart Failure. Card Fail Rev. 2017 Apr;3(1):7–11.

104. Luu JM, Schmidt A, Flewitt J, Mikami Y, Ter Keurs H, Friedrich MG. Cardiovascular risk is associated with a transmural gradient of myocardial oxygenation during adenosine infusion. Eur Heart J Cardiovasc Imaging. 2019 Nov 1;20(11):1287–95.

105. Null N, Cerqueira MD, Weissman NJ, Dilsizian V, Jacobs AK, Kaul S, et al. Standardized Myocardial Segmentation and Nomenclature for Tomographic Imaging of the Heart. Circulation. 2002 Jan 29;105(4):539–42.

106. Termeer M, Bescós JO, Breeuwer M, Vilanova A, Gerritsen F. Patient-specific mappings between myocardial and coronary anatomy. In Schloss Dagstuhl - Leibniz-Zentrum fuer Informatik GmbH, Wadern/Saarbruecken, Germany; 2010 [cited 2022 Apr 28]. Available from: http://drops.dagstuhl.de/opus/volltexte/2010/2705/

107. Mandrekar JN. Receiver operating characteristic curve in diagnostic test assessment. J Thorac Oncol. 2010 Sep;5(9):1315–6.

108. Koo TK, Li MY. A Guideline of Selecting and Reporting Intraclass Correlation Coefficients for Reliability Research. J Chiropr Med. 2016 Jun;15(2):155–63.

109. Angleys H, Jespersen SN, Østergaard L. The effects of capillary transit time heterogeneity on the BOLD signal. Hum Brain Mapp. 2018 Jun;39(6):2329–52.

110. Bernhardt P, Manzke R, Bornstedt A, Gradinger R, Spiess J, Walcher D, et al. Blood oxygen level-dependent magnetic resonance imaging using T2-prepared steady-state free-precession imaging in comparison to contrast-enhanced myocardial perfusion imaging. Int J Cardiol. 2011 Mar 17;147(3):416–9.